Sequential Energy and Electron Transfer in an Artificial Reaction Center: Formation of a Long-Lived Charge-Separated State

C. Luo,[†] D. M. Guldi,*[,†] H. Imahori,*[,‡] K. Tamaki,[§] and Y. Sakata[§]

Contribution from the Radiation Laboratory, University of Notre Dame, Notre Dame, Indiana 46556, Department of Material and Life Science, Graduate School of Engineering, Osaka University, 2-1 Yamada-oka, Suita, Osaka 565-0871, Japan, and The Institute of Scientific and Industrial Research, Osaka University, 8-1 Mihoga-oka, Ibaraki, Osaka 567-0047, Japan

Received November 9, 1999. Revised Manuscript Received February 9, 2000

Abstract: A novel molecular triad, representing an artificial reaction center, was synthesized via linking a fullerene moiety to an array of two porphyrins (i.e., a zinc tetraphenyl porphyrin (ZnP) and a free base tetraphenyl porphyrin (H_2P)). In this ZnP−H_2P−C_{60} triad, the ZnP performs as an antenna molecule, transferring its singlet excited state energy to the energetically lower lying H_2P. In benzonitrile, this energy transfer ($k = 1.5 \times 10^{10}$ s^{-1}) is followed by a sequential electron-transfer relay evolving from the generated singlet excited state of H_2P to yield ZnP−$H_2P^{\bullet+}$−$C_{60}^{\bullet-}$ and subsequently ZnP$^{\bullet+}$−H_2P−$C_{60}^{\bullet-}$ with rate constants of 7.0×10^9 s^{-1} and 2.2×10^9 s^{-1}, respectively. The final charge-separated state, formed in high yield (0.4), gives rise to a remarkable lifetime of 21 μs in deoxygenated benzonitrile and decays directly to the singlet ground state. In contrast, in nonpolar toluene solutions the deactivation of the porphyrin chromophores (ZnP and H_2P) takes place via singlet−singlet energy transfer leading to the fullerene singlet excited state. This stems from the unfavorable free energy changes for an intramolecular electron-transfer event in toluene from the singlet excited state of H_2P to the adjacent fullerene acceptor.

Introduction

The principal aspects of the primary photochemical energy conversion process in photosynthesis have been thoroughly investigated in recent years, starting with the isolation and full characterization of the photosynthetic reaction center.[1] In particular, there is a sequence of events that separate charges across a membrane within a nanosecond.[2−4] These events are a fast energy transfer from the photoexcited antenna molecule to the photosynthetic reaction center followed by two successive one-electron reduction steps.[5,6] It should be noted that one of the key factors, to achieve a near-unity quantum efficiency for the charge separation, implements small reorganization energies for the initial photoinduced electron transfer from the special pair bacterial chlorophyll to ubiquinone.[7] In this context, a vast number of artificial systems were designed with the purpose of mimicking these primary events.[8−21] However, the exquisite selectivity and control of electron transfer of the photosynthetic reaction center has not yet been reached in these model systems.

With the advent of fullerenes, a new three-dimensional electron acceptor became available that displays appealing characteristics.[22,23] Most important, fullerenes have a remarkably low reorganization energy, associated with their electron transfer (ET) reaction, which results from the rigid, confined structure of the carbon network.[24,25] Small resonance-Raman shifts[26] and small Stokes shifts,[27] noticed in reduction and excitation experiments, point to the similarity of the fullerene nuclear configurations in the excited, reduced, and ground state. These effects are beneficial to decelerate the energy-wasting back-electron transfer (BET)[28] relative to 2-dimensional electron acceptors, which in general have less rigid structures and, thus, higher reorganization energies than 3-dimensional fullerenes,

* Author to whom correspondence may be sent. E-mail: guldi.1@nd.edu.
† University of Notre Dame.
‡ Graduate School of Engineering, Osaka University. E-mail: imahori@ap.chem.eng.osaka-u.ac.jp.
§ The Institute of Scientific and Industrial Research, Osaka University.

(1) Deisenhofer, J.; Epp, O.; Miki, K.; Huber, R.; Michel, H. *J. Mol. Biol.* **1984**, *180*, 385.
(2) McDermott, G.; Prince, S. M.; Freer, A. A.; Hawethornthwaite-Lawless, A. M.; Paiz, M. Z.; Cogdell, R. J.; Isaacs, N. W. *Nature* **1995**, *374*, 517.
(3) Stowell, M. H. B.; McPhillips, T. M.; Rees, D. C.; Soltis, S. M.; Abresch, E.; Feher, G. *Science* **1997**, *276*, 812.
(4) Beratan, D. N.; Onuchic, J. N.; Winkler, J.; Gray, H. *Science* **1992**, *258*, 1740.
(5) Vermaas, W. F. J. *Science* **1994**, *263*, 545.
(6) Steffen, M. A.; Lao, K. Q.; Boxer, S. G. *Science* **1994**, *264*, 810.
(7) Moser, C. C.; Keske, J. M.; Warncke, K.; Farid, R. S.; Dutton, P. L. *Nature* **1992**, *355*, 796.
(8) Maruyama, K.; Osuka, A. *Pure Appl. Chem.* **1990**, *62*, 1511.
(9) Gust, D.; Moore, T. A. *Science* **1989**, *244*, 35.
(10) Gust, D.; Moore, T. A. *Adv. Photochem.* **1991**, *16*, 1.
(11) Gust, D.; Moore, T. A. *Top. Curr. Chem.* **1991**, *159*, 103.
(12) Gust, D.; Moore, T. A.; Moore, A. L. *Acc. Chem. Res.* **1993**, *26*, 198.
(13) Wasielewski, M. R. *Chem. Rev.* **1992**, *92*, 435.
(14) Paddon-Row, M. N. *Acc. Chem. Res.* **1994**, *27*, 18.
(15) Sutin, N. *Acc. Chem. Res.* **1983**, *15*, 275.
(16) Bard, A. J.; Fox, M. A. *Acc. Chem. Res.* **1995**, *28*, 141.
(17) Meyer, T. J. *Acc. Chem. Res.* **1989**, *22*, 163.
(18) Harriman, A.; Kubo, Y.; Sessler, J. L. *J. Am. Chem. Soc.* **1992**, *114*, 388.
(19) Piotrowiak, P. *Chem. Soc. Rev.* **1999**, *28*, 143.
(20) Galoppini, E.; Fox, M. A. *J. Am. Chem. Soc.* **1997**, *119*, 5277.
(21) Blanco, M.-J.; Jimeńez, M. C.; Chambron, J.-C.; Heitz, V.; Linke, M.; Sauvage, J.-P. *Chem. Soc. Rev.* **1999**, *28*, 293.
(22) Kroto, H. W.; Heath, J. R.; O'Brien, S. C.; Curl, R. F.; Smalley, R. E. *Nature* **1985**, *318*, 162.
(23) *Fullerenes and Related Structures*; Hirsch, A., Ed.; Springer: Berlin, Vol. 199, 1999.
(24) Guldi, D. M.; Asmus, K.-D. *J. Am. Chem. Soc.* **1997**, *119*, 5744.
(25) Imahori, H.; Hagiwara, K.; Akiyama, T.; Aoki, M.; Taniguchi, S.; Okada, T.; Shirakawa, M.; Sakata, Y. *Chem. Phys. Lett.* **1996**, *263*, 545.
(26) McGlashen, M. L.; Blackwood, M. E.; Spiro, T. G. *J. Am. Chem. Soc.* **1993**, *115*, 2074.
(27) Guldi, D. M.; Asmus, K.-D. *J. Phys. Chem. A* **1997**, *101*, 1472.
(28) Marcus, R. A. *J. Phys. Chem.* **1956**, *24*, 966.

10.1021/ja993959z CCC: $19.00
Published on Web 06/30/2000

and this makes them ideal candidates for model systems.[29−34] This is of great interest for modulating the rates and yields of charge separation versus charge recombination, in particular, in relation to conventionally employed acceptors, such as quinones A and B in the reaction center. Consequently, fullerenes emerged as ideal candidates for novel model donor−acceptor systems.

Molecular calculations regarding the electronic configuration of fullerenes have revealed that in C_{60} an energy gap of ~1.8 eV separates a 3-fold degenerate LUMO from a lower lying 5-fold degenerate HOMO.[35,36] The small energy gap underlines the remarkable electron-accepting features of these carbon spheres. In line with this, a low redox potential (associated with the first reduction step) of −440 mV versus SCE is reported, for example, in dichloromethane solutions.[37]

By far the largest number of C_{60}-based donor−acceptor systems studied to date are based on employing porphyrins as antenna molecules to ensure the efficient light capture in the visible region of the spectrum.[29−34,38−45] One of the first reported C_{60}-based donor−acceptor systems is H_2P-C_{60} and the analogue $ZnP-C_{60}$ dyads, in which the pigments are linked via an unusual bicyclic spacer.[38a] The fluorescence lifetime measurements suggested photoinduced ET in these systems. First direct evidence for ET in donor-linked fullerenes also stems from time-resolved transient absorption studies regarding a $ZnP-C_{60}$ dyad, in which the two chromophores are separated by a phenyl spacer.[44a]

The role played by the spacer is not just limited to structural concerns, but more importantly, its chemical nature influences the electronic communication between the electron acceptor (i.e., fullerene) and photoexcited electron donor (i.e., ZnP). As a leading example for a short-spaced dyad, the $\pi-\pi$ stacked porphyrin−fullerene dyad ($ZnP-C_{60}$) should be cited,[39a] whose ET and BET dynamics helped to establish the following fundamental aspect:[45b] The presence of a "Marcus-inverted" region for BET was found, based on (i) the photoactivation of an intramolecular ET in a variety of solvents and (ii) the formation of a highly energetic charge-separated state. Similar observations stem from a series of parachute-shaped dyads (e.g., $ZnP-C_{60}$ and H_2P-C_{60})[42e] as well as $ZnP-C_{60}$ dyads with a variety of phenyl spacers.[25,44b]

One approach to slowing down charge recombination is to increase the distance between the donor and acceptor by means of using spacer units of increasing size.[40] For example, a long-range photoinduced electron transfer was reported in a $ZnP-C_{60}$ dyad, in which the two redox active moieties are separated by a saturated norbornylogous bridge nine σ bonds in length.[40a] The lifetime of the radical ion pair in the "norbornylogous" bridged dyad measures an impressively 420 ns[40a] and clearly discloses a significant improvement relative to the short-spaced analogues. (e.g., the $\pi-\pi$ stacked $ZnP-C_{60}$: 38 ps in benzonitrile[45b]).

The above-summarized dyad concept (i.e., $ZnP-C_{60}$) was further developed by linking a carotenoid polyene (C) to a H_2P-C_{60} dyad, constituting the first molecular triad published (e.g., $C-H_2P-C_{60}$).[38d,h] In this system the spatial separation between the individual components is, however, rather short and, in turn, limits the stability of the charge-separated state. A similar linkage was chosen for the design of an artificial reaction center, namely, the sequence of energy and electron transfer. In particular, in an elaborated C_{60}-based hexad, $(ZnP)_3-ZnP-H_2P-C_{60}$, star-shaped aligned porphyrins (i.e., four ZnP linked to a H_2P) serve as a multichromophoric antenna system.[38f]

In the present work we developed a concept in which we have linked the fullerene acceptor covalently to an array of two porphyrin moieties, namely, a tetraphenyl porphyrin free base (H_2P) and the corresponding zinc complex (ZnP), to form a novel artificial reaction center, as shown in Figure 1. Importantly, the center-to-center distances in **$ZnP-H_2P-C_{60}$** were estimated to be 18.0 and 36.1 Å for the H_2P/C_{60} and ZnP/C_{60}

(29) Martín, N.; Sánchez, L.; Illescas, B.; Pérez, I. *Chem. Rev.* **1998**, *98*, 2527.
(30) Imahori, H.; Sakata, Y. *Adv. Mater*. **1997**, *9*, 537.
(31) Prato, M. *J. Mater. Chem*. **1997**, *7*, 1097.
(32) Diederich, F.; Gomez-Lopez, M. *Chem. Soc. Rev*. **1999**, *28*, 263.
(33) Imahori, H.; Sakata, Y. *Eur. J. Org. Chem*. **1999**, 2445.
(34) Guldi, D. M. *Chem Commun*. **2000**, 321.
(35) Haddon, R. C. *Acc. Chem. Res.* **1988**, *21*, 243.
(36) Haddon, R. C. *Science* **1993**, *261*, 1545.
(37) Echegoyen L.; Echegoyen, L. E. *Acc. Chem. Res*. **1998**, *31*, 593.
(38) (a) Liddell, P. A.; Sumida, J. P.; Macpherson, A. N.; Noss, L.; Seely, G. R.; Clark, K. N.; Moore, A. L.; Moore, T. A.; Gust, D. *Photochem. Photobiol*. **1994**, *60*, 537. (b) Kuciauskas, D.; Lin, S.; Seely, G. R.; Moore, A. L.; Moore, T. A.; Gust, D.; Drovetskaya, T.; Reed, C. A.; Boyd, P. D. W. *J. Phys. Chem*. **1996**, *100*, 15926. (c) Gust, D.; Moore, T. A.; Moore, A. L. *Res. Chem. Intermed*. **1997**, *23*, 621. (d) Liddell, P. A.; Kuciauskas, D.; Sumida, J. P.; Nash, B.; Nguyen, D.; Moore, A. L.; Moore, T. A.; Gust, D. *J. Am. Chem. Soc*. **1997**, *119*, 1400. (e) Gust, D.; Moore, T. A.; Moore, A. L. *Pure Appl. Chem*. **1998**, *70*, 2189. (f) Kuciauskas, D.; Liddell, P. A.; Lin, S.; Johnson, T. E.; Weghorn, S. J.; Lindsey, J. S.; Moore, A. L.; Moore, T. A.; Gust, D. *J. Am. Chem. Soc*. **1999**, *121*, 8604. (g) Imahori, H.; Cardoso, S.; Tatman, D.; Lin, S.; Noss, L.; Seely, G. R.; Sereno, L.; de Silber, J. C.; Moore, T. A.; Moore, A. L.; Gust, D. *Photochem. Photobiol*. **1995**, *62*, 1009. (h) Carbonera, D.; Di Valentin, M.; Corvaja, C.; Agostini, G.; Giacometti, G.; Liddell, P. A.; Kuciauskas, D.; Moore, A. L.; Moore, T. A.; Gust, D. *J. Am. Chem. Soc*. **1998**, *120*, 4398.
(39) (a) Dietel, E.; Hirsch, A.; Eichborn, E.; Rieker, A.; Hackbarth, S.; Röder, B. *Chem. Commun*. **1998**, 1981. (b) Dietel, E.; Hirsch, A.; Zhou, J.; Rieker, A. *J. Chem. Soc., Perkin Trans. 2* **1998**, 1357. (c) Camps, X.; Dietel, E.; Hirsch, A.; Pyo, S.; Echegoyen, L.; Hackbarth, S.; Röder, B. *Chem. Eur. J*. **1999**, *5*, 2362.
(40) (a)Bell, T. D. M.; Smith, T. A.; Ghiggino, K. P.; Ranasinghe, M. G.; Shephard, M. J.; Paddon-Row, M. N. *Chem. Phys. Lett*. **1997**, *268*, 223. (b) Paddon-Row, M. N. *Fullerene Sci. Technol*. **1999**, *7*, 1151. (c) Shephard, M. J.; Paddon-Row: M. N. *Aust. J. Chem*. **1996**, *49*, 395.
(41) (a) Nierengarten, J.-F.; Schall, C.; Nicoud, J.-F. *Angew. Chem., Int. Ed*. **1998**, *37*, 1934. (b) Nierengarten, J.-F.; Oswald, L.; Nicaud, J.-F. *Chem. Commun*. **1998**, 1545. (c) Bourgeois, J.-P.; Diederich, F.; Echegoyen, L.; Nierengarten, J.-F. *Helv. Chim. Acta* **1998**, *81*, 1835. (d) Armaroli, N.; Diederich, F.; Echegoyen, L.; Habicher, T.; Flamigni, L.; Marconi, G.; Nierengarten, J.-F. *New J. Chem*. **1999**, *23*, 77.
(42) (a) Safonov, I. G.; Baran, P. S.; Schuster, D. I. *Tetrahedron Lett*. **1997**, *38*, 8133. (b) Baran, P. S.; Monaco, R. R.; Khan, A. U.; Schuster, D. I.; Wilson, S. R. *J. Am. Chem. Soc*. **1997**, *119*, 8363. (c) Fong, R.; Schuster, D. I.; Wilson, S. R. *Org. Lett.* **1999**, *1*, 729. (d) Cheng, P.; Wilson, S.; Schuster, D. I. *Chem. Commun*. **1999**, 89. (e) Schuster, D. I.; Cheng, P.; Wilson, S. R.; Prokhorenko, V.; Katterle, M.; Holzwarth, A. R.; Braslavsky, S. E.; Klihm, G.; Williams, R. M.; Luo, C. *J. Am. Chem. Soc*. **1999**, *121*, 11599.
(43) (a) Helaja, J.; Tauber, A. Y.; Abel, Y.; Tkachenko, N. V.; Lemmetyinen, H.; Kilpeläinen, I.; Hynninen, P. H. *J. Chem. Soc., Perkin Trans. 1* **1999**, 2403. (b) Tkachenko, N. V.; Rantala, L.; Tauber, A. Y.; Helaja, J.; Hynninen, P. H.; Lemmetyinen, H. *J. Am. Chem. Soc*. **1999**, *121*, 9378.
(44) (a) Imahori, H.; Hagiwara, K.; Akiyama, T.; Taniguchi, S.; Okada, T.; Sakata, Y. *Chem. Lett*. **1995**, 265. (b) Imahori, H.; Hagiwara, K.; Aoki, M.; Akiyama, T.; Taniguchi, S.; Okada, T.; Shirakawa, M.; Sakata, Y. *J. Am. Chem. Soc*. **1996**, *118*, 11771. (c) Imahori, H.; Yamada, K.; Hasegawa, M.; Taniguchi, S.; Okada, T.; Sakata, Y. *Angew. Chem. Int. Ed. Engl*. **1997**, *36*, 2626. (d) Higashida, S.; Imahori, H.; Kaneda, T.; Sakata, Y. *Chem. Lett*. **1998**, 605. (e) Tamaki, K.; Imahori, H.; Nishimura, Y.; Yamazaki, I.; Shimomura, A.; Okada, T.; Sakata, Y. *Chem. Lett*. **1999**, 227. (f) Imahori, H.; Ozawa, S.; Ushida, K.; Takahashi, M.; Azuma, T.; Ajavakom, A.; Akiyama, T.; Hasegawa, M.; Taniguchi, S.; Okada, T.; Sakata, Y. *Bull. Chem. Soc. Jpn*. **1999**, *72*, 485. (g) Fujitsuka, M.; Ito, O.; Imahori, H.; Yamada, K.; Yamada, H.; Sakata, Y. *Chem. Lett*. **1999**, 721. (h) Yamada, K.; Imahori, H.; Nishimura, Y.; Yamazaki, I.; Sakata, Y. *Chem. Lett*. **1999**, 895.
(45) (a) Da Ros, T.; Prato, M.; Guldi, D. M.; Alessio, E.; Ruzzi, M.; Pasimeni, L. *Chem. Commun*. **1999,** 635. (b) Guldi, D. M.; Luo, C.; Prato, M.; Dietel, E.; Hirsch, A. *Chem. Commun*. **2000**, 373. (c) Guldi, D. M.; Luo, C.; Prato, M.; Da Ros, T.; Dietel, E.; Hirsch, A. *Chem. Commun*. **2000**, 375. (d) Da Ros, T.; Prato, M.; Guldi, D. M.; Ruzzi, M.; Pasimeni, L. Submitted for publication.

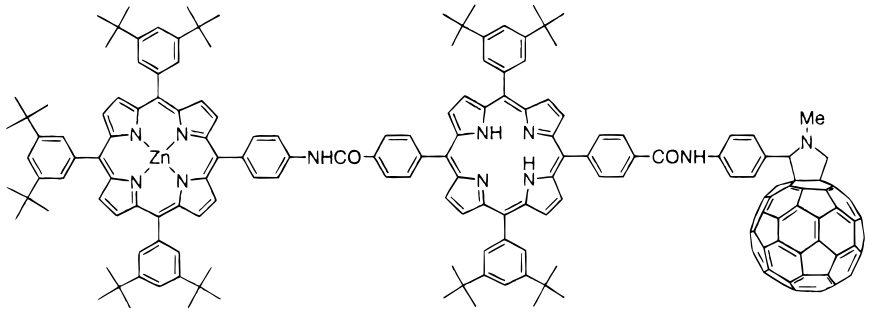

ZnP-H_2P-C_{60}

Figure 1. Structure of **ZnP**−**H_2P**−**C_{60}** triad.

separations, respectively, using CPK modeling. The ZnP chromophore is believed to act herein as the antenna molecule, which transfers its singlet excited-state energy to the adjacent H_2P chromophore. Furthermore, a sequential electron-transfer relay will evolve from the generated singlet excited state of H_2P, injecting an electron into the electron-accepting fullerene, to yield $ZnP-H_2P^{\bullet+}-C_{60}^{\bullet-}$ and subsequently $ZnP^{\bullet+}-H_2P-C_{60}^{\bullet-}$.

Earlier some of us reported on the time-resolved fluorescence studies of this system, which revealed a rapid quenching of the antenna fluorescence in the reference dyads **ZnP**−**C_{60}** and **H_2P**−**C_{60}** (Scheme 3) and also in the molecular triad **ZnP**−**H_2P**−**C_{60}**.[46] Now, we wish to present the complete characterization of the transient intermediates associated with the quenching of the porphyrin emission by means of transient absorption spectroscopy. We also provide the rate constants for all of the individual events involved, starting from the initial quenching processes to the decay kinetics of the final photoproducts.

Results and Discussion

Synthesis:[46] The preparation of **ZnP**−**H_2P**−**C_{60}** and the reference dyads **ZnP**−**H_2P**, **H_2P**−**C_{60}** and **ZnP**−**C_{60}** was carried out as shown in Schemes 1−3. Important synthetic intermediates **4** and **5** were prepared by the condensation of dipyrromethane **1** with 3,5-di-*tert*-butylbenzaldehyde in the presence of BF_3OEt_2, followed by base hydrolysis of **2** and **3**, respectively (Scheme 1). The key features for the synthesis of **ZnP**−**H_2P**−**C_{60}** and **ZnP**−**H_2P** involve selective insertion of the central zinc atom into the diporphyrin and its protection from the demetalation. Therefore, after completion of the insertion all of the procedures were carried out under neutral or basic conditions. The free-base porphyrin carboxylic diacid **4** was converted to the corresponding bis(acid chloride) **6** by treatment with $SOCl_2$. Amino zincporphyrin **7** was synthesized from the corresponding freebase porphyrin, whereas 4-*tert*-butyldimethylsiloxymethylaniline **9** was obtained by protection of the hydroxymethyl group in 4-nitrobenzyl alcohol and subsequent reduction of the nitro group in **8** (Scheme 2). Cross-condensation of **6** with **7** and **9** in benzene in the presence of pyridine afforded a mixture of porphyrins. The desired diporphyrin **10** was isolated in 34% by tedious chromatographic separation. Deprotection of *tert*-butyldimethylsilyl group in **10** with *n*-Bu_4NF gave **11**, which was oxidized using activated MnO_2 to yield **12**. $ZnP-H_2P-C_{60}$ was obtained by 1,3-dipolar cycloaddition using **12**, *N*-methylglycine, and C_{60} in toluene in 79% yield. **ZnP**−**H_2P** was synthesized from **6**, **7**, and 4-hexadecylaniline by the same method as described for **ZnP**−**H_2P**−**C_{60}** (Scheme 2). **H_2P**−**C_{60}** was obtained by condensation of **5** with **13**, followed by acid hydrolysis of **14** and 1,3-dipolar cycloaddition using **15**, *N*-methylglycine, and C_{60} in toluene (Scheme 3). Preparation of **ZnP**−**C_{60}** was carried out by treatment of **H_2P**−**C_{60}** with $Zn(OAc)_2$. The single chromophore references **ZnP**, **H_2P**, and **C_{60}**−**Ar** were also prepared (Figure 2). Their structures were verified by spectroscopic analyses including ^{1}H NMR and MALDI-TOF mass spectra (see Experimental Section).

Scheme 1

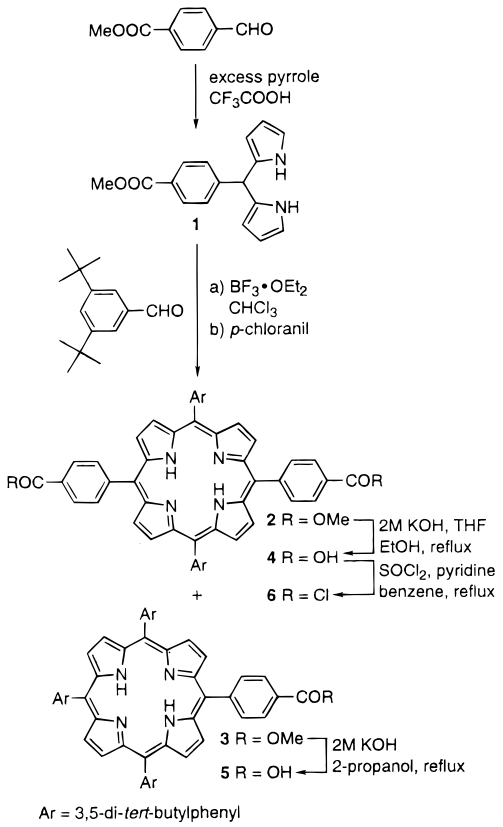

The absorption spectrum of **ZnP**−**H_2P**−**C_{60}** in benzonitrile is almost a linear combination of the spectra of **ZnP**, **H_2P**, and **C_{60}**−**Ar**, indicating no significant interactions among the three chromophores in the ground state. In principle, the absorption features of the two porphyrin chromophores in the visible region are much stronger than that of the fullerene moiety.

Electrochemical Properties and Thermodynamic Free Energy Changes. The redox potentials of **ZnP**−**H_2P**−**C_{60}**, **ZnP**−**H_2P**, **ZnP**−**C_{60}**, **H_2P**−**C_{60}**, **ZnP**, **H_2P**, and **C_{60}**−**Ar** were measured by differential pulse voltammetry in benzonitrile using

(46) Tamaki, K.; Imahori, H.; Nishimura, Y.; Yamazaki, I.; Sakata, Y. *Chem. Commun.* **1999**, 625.

Scheme 2

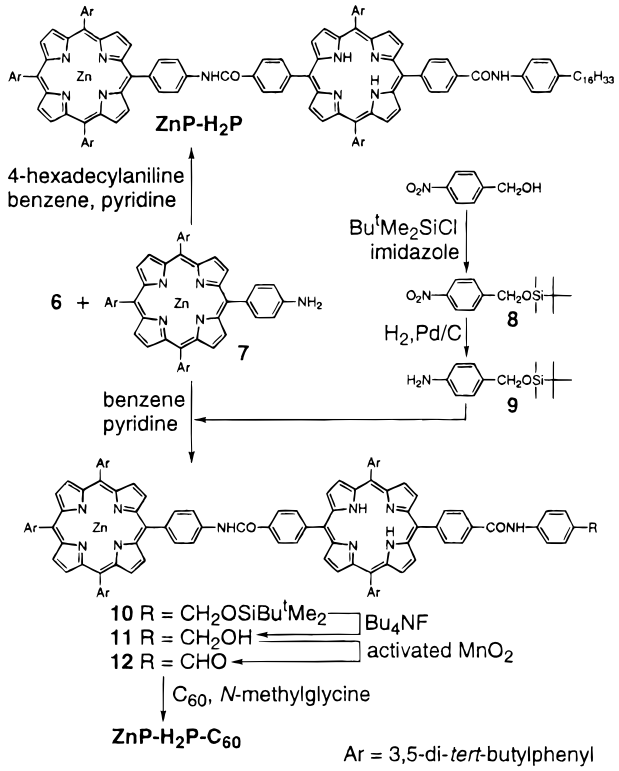

Scheme 3

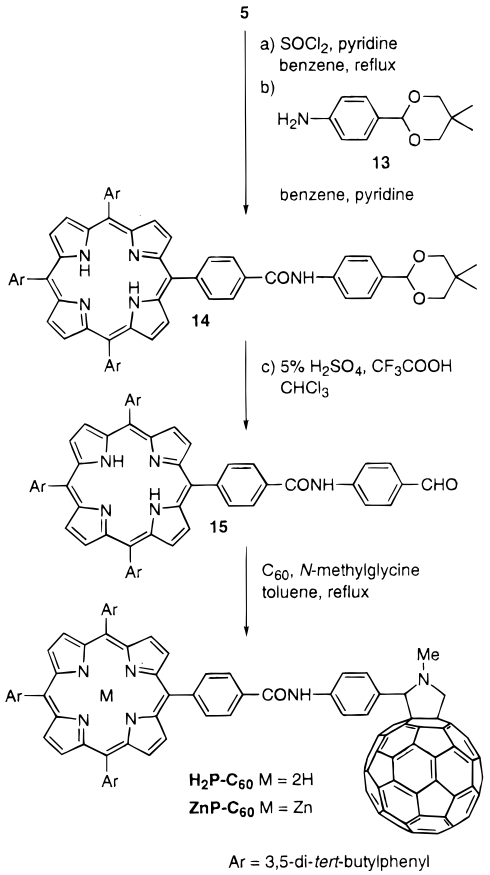

0.1 M *n*-Bu_4NPF_6 as supporting electrolyte. The results are summarized in Table 1. The potentials of **ZnP**−**H₂P**−**C₆₀** (+0.30, +0.59 V, −1.04, vs Fc/Fc^+) can be roughly explained by the sum of **ZnP**, **H₂P**, and **C₆₀**−**Ar** ($E_{1/2}$ ($ZnP^{\bullet+}$/ZnP) = +0.29 V; $E_{1/2}$ ($H_2P^{\bullet+}/H_2P$) = +0.49 V; $E_{1/2}$ ($C_{60}/C_{60}^{\bullet-}$) = −1.05 V vs Fc/Fc^+), implying the weak electronic coupling among the three moieties. The difference in the substituents in **ZnP**−**H₂P**−**C₆₀** and **H₂P** may be responsible for the shift in the first oxidation potential of the freebase porphyrin moieties. Tables 1 and 2 and Scheme 4 show the energy levels of the locally excited singlet states of the three moieties (i.e., ZnP, H_2P, and C_{60}) and the free-energy changes. The energies of the 0−0 transition (ΔE_{0-0}) between the S_1 and the S_0 state were determined by averaging the energies of the corresponding (0, 0) peaks in the fluorescence and the absorption bands. Free energy changes, $-\Delta G_{CS}$ and $-\Delta G_{CR}$, were calculated by the Rehm−Weller and Born equation.[47,48] E_{OX} and E_{RED} are the half-wave potentials of the one-electron oxidation step of the porphyrin and one-electron reduction step of C_{60}, respectively, in benzonitrile. ΔG_S is the correction term for the effects of solvent polarity as well as the Coulombic energy between donor radical cation and acceptor radical anion. In benzonitrile the Born equation may estimate the correct values for ΔG_S, whereas in toluene that was tentatively used due to the overestimation of the nonpolarity of toluene. The center-to-center distances (R_{D-A}) were determined from CPK modeling using CAChe (version 3.7 CAChe Scientific, 1994).

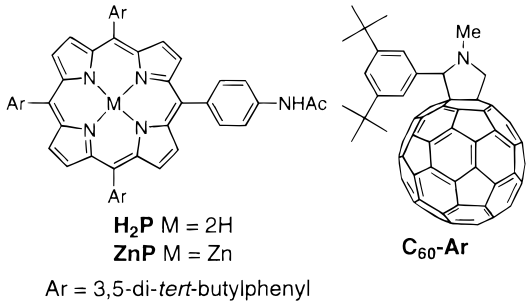

Figure 2. Structures of **ZnP**, **H₂P**, and **C₆₀**−**Ar** references.

Time-Resolved Absorption Studies. To characterize the transient intermediates involved in the rapid deactivation of the metalloporphyrins, a number of fast spectroscopic techniques were employed. In particular, transient absorption measurements were carried out following either pico- or nanosecond laser excitation (337 or 532 nm) of the **ZnP**−**H₂P**−**C₆₀** triad and the corresponding reference compounds in solvents of different polarity. These data are further complemented by time-resolved fluorescence lifetime measurements, published recently.[46] The pump wavelength of 532 nm was chosen in these experiments, to guarantee the excitation into both the zinc porphyrin and free base porphyrin ($\pi-\pi^*$) visible transitions, namely, the *Q*-bands, rather than excitation of the fullerene moiety.

ZnP and H₂P. Eighteen picosecond excitation of either the free base tetraphenyl porphyrin (**H₂P**) or the corresponding zinc complex (**ZnP**) resulted in characteristic absorption changes in the 500−810 nm range. In particular, a net decrease of the absorption was observed around 540 nm, a region, which is dominated by strong ZnP and H_2P ground-state absorption. This suggests consumption of the porphyrin as a result of converting the porphyrin singlet ground states to the corresponding singlet excited states, $^1*(\pi-\pi^*)$ZnP and $^1*(\pi-\pi^*)H_2P$. An immediately formed absorption accompanies this porphyrin bleaching. For example, the $^1*(\pi-\pi^*)H_2P$ exhibits a new absorption band between 660 and 730 nm, a region in which the $^1*(\pi-\pi^*)$ZnP absorbs, however, very weakly. The singlet excited-state absorp-

(47) Weller, A. *Z. Phys. Chem.* **1982**, *132*, 93.
(48) Gaines, G. L. I.; O'Neil, M. P.; Svec, W. A.; Niemczyk M. P.; Wasielewski, M. R. *J. Am. Chem. Soc.* **1991**, *113*, 719.

Table 1. Redox Potentials[a] and Thermodynamic Driving Force in Fullerene−Porphyrin References, Dyads, and Triad

	redox potential			free energy change: benzonitrile				free energy change: toluene			
	$H_2P^{\bullet+}/H_2P^{\bullet+}$ [V]	$ZnP^{\bullet+}/ZnP$ [V]	$C_{60}/C_{60}^{\bullet-}$ [V]	$-\Delta G_{CS}$[b] [eV]	$-\Delta G_{CR1}$[b] [eV]	$-\Delta G_{CSH}$[c] [eV]	$-\Delta G_{CR2}$[c] [eV]	$-\Delta G_{CS}$[b] [eV]	$-\Delta G_{CR1}$[b] [eV]	$-\Delta G_{CSH}$[c] [eV]	$-\Delta G_{CR2}$ [eV]
ZnP−H$_2$P−C$_{60}$	0.59	0.30	−1.04	0.29	1.60	0.28	1.32	−0.56	2.46		2.34
H$_2$P−C$_{60}$	0.55		−1.04	0.33	1.56			−0.52	2.42	0.12	
ZnP−C$_{60}$		0.34	−1.04	0.69	1.35			−0.13	2.21		
ZnP−H$_2$P	0.59	0.30									
H$_2$P	0.49										
ZnP		0.29									
C$_{60}$−Ar			−1.05								

[a] Redox potentials were measured in benzonitrile (0.1 M Bu_4NPF_6, vs Fc/Fc^+) by differential pulse voltammetry with a sweep rate of 10 mVs^{-1}, using a glassy carbon working electrode, a platinum wire counter electrode, and a Ag/AgCl (saturated KCl) reference electrode. [b] $-\Delta G_{CS}$ and $-\Delta G_{CR1}$ denote the free-energy changes for an electron transfer from $^1*(\pi-*\pi)ZnP/^1*(\pi-*\pi)H_2P$ to C_{60}, and from $C_{60}^{\bullet-}$ to $ZnP^{\bullet+}/H_2P^{\bullet+}$, respectively. [c] $-\Delta G_{CSH}$ and $-\Delta G_{CR2}$ denote the free-energy changes for an electron transfer from ZnP to the $H_2P^{\bullet+}$, and from $C_{60}^{\bullet-}$ to $ZnP^{\bullet+}$, respectively. (see refs 44b, 47, 48). $-\Delta G_{CS} = \Delta E_{0-0} - (-\Delta G_{CR})$; $-\Delta G_{CR} = E_{OX} - E_{RED} + \Delta G_S$; $\Delta G_S = e^2/(4\pi\epsilon_0))$ $[(1/(2R_+) + 1/(2R_-) - 1/R_{D-A})\ 1/\epsilon_S - (1/(2R_+) + 1/(2R_-))\ 1/\epsilon_R]$; $E_{OX} = E_{1/2}$ ($D^{\bullet+}/D$); $E_{RED} = E_{1/2}$ ($A/A^{\bullet-}$); R_+ = radius donor (5 Å); R_- = radius acceptor (4.4 Å); R_{D-A} = center-to-center distance; ϵ_S = dielectric constant of solvent used for photophysical studies; $\epsilon_S = 2.38$ (toluene) and $\epsilon_S = 25.2$ (benzonitrile) ϵ_R = dielectric constant of solvent used for measuring the redox potentials; ΔE_{0-0} = excited-state energy of chromophore.

Table 2. Energies, Lifetimes, and Quantum Yields of Fullerene−Porphyrin References, Dyads, and Triads in Toluene

compd	energy: singlet excited state [eV]	lifetime: singlet excited state	energy: triplet excited state [eV]	lifetime: triplet excited state	quantum yield: triplet excited state
***H$_2$P**	1.90	10.1 ns	1.40	380 μs	0.82
***ZnP**	2.08	2.5 ns	1.53	44 μs	0.88
***C$_{60}$−Ar**	1.75	1.8 ns	1.50	25 μs	0.98
***H$_2$P−C$_{60}$**	1.90	67 ps			0
H$_2$P−*C$_{60}$	1.75	1.8 ns	1.50	4.2 μs	0.83
***H$_2$P−C$_{60}$**[a]			1.40	240 μs	0.54
***ZnP−H$_2$P**	2.08	79 ps			0
ZnP−*H$_2$P	1.90	10.1 ns	1.40	380 μs	0.76
***ZnP−C$_{60}$**	2.08	58 ps			
ZnP−*C$_{60}$	1.75	1.8 ns	1.50	25 μs	0.86
***ZnP−H$_2$P−C$_{60}$**	2.08	67 ps			0
ZnP−*H$_2$P−C$_{60}$	1.90	87 ps			
ZnP−H$_2$P−*C$_{60}$	1.75	1.8 ns	1.50	4.2 μs	0.71
ZnP−*H$_2$P−C$_{60}$[a]			1.40	240 μs	0.46

[a] Produced via intramolecular energy transfer.

Scheme 4

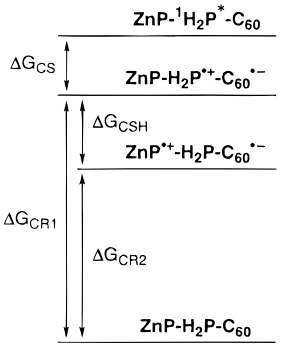

tion gives rise to singlet lifetimes of 10.1 ns and 2.5 ns for **H$_2$P** and **ZnP**, respectively. These are in excellent agreement with previously reported values and confirm the negligible effects stemming from the functionalization of the porphyrin periphery on the singlet excited-state properties.[45a,49−51] They also reveal a good agreement with the fluorescence lifetimes of the **H$_2$P** and **ZnP** chromophores in THF with values of 9.8 ns and 2.0 ns, respectively.[46]

$$ZnP \xrightarrow{h\nu} {}^1*ZnP \rightarrow {}^3*ZnP \quad (1)$$

$$H_2P \xrightarrow{h\nu} {}^1*H_2P \rightarrow {}^3*H_2P \quad (2)$$

Intersystem crossing is the predominant fate of these singlet excited states (see Table 2).[50,51] The accordingly formed triplet excited state of **H$_2$P** reveals a characteristic peak around 780 nm (Figure 3, spectrum a), while the absorption of the analogous **ZnP** is markedly shifted to the red (λ_{max} = 860 nm) (Figure 3, spectrum b). Again, the derived triplet lifetimes of 380 μs ($^3*(\pi-\pi*)H_2P$) and 44 μs ($^3*(\pi-\pi*)ZnP$) match those values reported earlier for a free base tetraphenylporphyrin and the corresponding zinc complex, respectively.[49] The energy levels of the singlet and triplet excited states, as derived from steady-state fluorescence and phosphorescence measurements are summarized, together with the associated lifetimes, in Table 2. The triplet quantum yields in these reference porphyrins were determined to be 0.82 and 0.88 for the free base and zinc complex, respectively, resembling already published values.[49] In the presence of molecular oxygen, the triplet excited states of both porphyrins experience a concentration-dependent deactivation process with oxygen concentration varying between 0.9 and 4.5 mM. Bimolecular rate constants of 6.6×10^8 M^{-1} s^{-1} and 1.06×10^9 M^{-1} s^{-1} for $^3*(\pi-\pi*)ZnP$ and

(49) (a) Murov, S. L.; Carmichael, I.; Hug, G. L. *Handbook of Photochemistry*; Marcel Dekker Inc.: New York, 1993. (b) Hoffman, M. Z.; Bolletta, F.; Moggi, L.; Hug, G. L. *J. Phys. Chem. Ref. Data* **1989**, *18*, 219.

(50) Rodriguez, J.; Kirmaier, C.; Holten, D. *J. Am. Chem. Soc.* **1989**, *111*, 6500.

(51) Kalyanasundaram, K. *Photochemistry of Polypyridine and Porphyrin Complexes*; Academic Press: London, 1992.

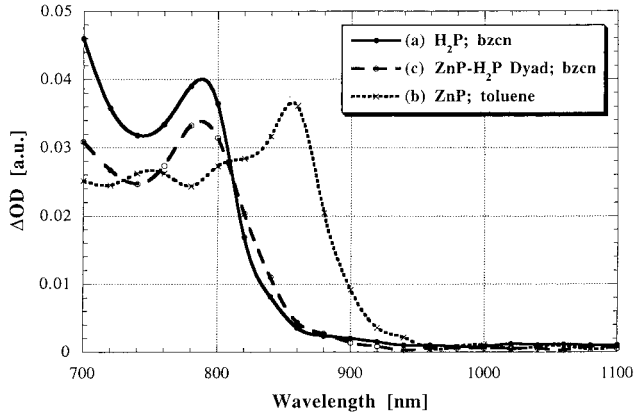

Figure 3. Differential absorption spectra obtained 50 ns upon nanosecond flash photolysis (532 nm) of ~10^{-5} M solutions of **H_2P** in nitrogen saturated benzonitrile (a) (—), **ZnP** in nitrogen saturated toluene (b) (- - -), **ZnP−H_2P** dyad in nitrogen saturated benzonitrile (c) (— — —).

Table 3. Reactivity of Photolytically Generated Species in Fullerene−Porphyrin Dyads and Triad with Molecular Oxygen

compd	reactive species	solvent	k_{OXYGEN} [M^{-1} s^{-1}]
ZnP	*ZnP	benzonitrile	6.6×10^8
H_2P	*H_2P	benzonitrile	1.06×10^9
H_2P	*H_2P	toluene	9.1×10^8
C_{60}−Ar	*C_{60}−Ar	toluene	1.0×10^9
ZnP−C_{60}	ZnP−*C_{60}	toluene	9.8×10^8
ZnP−C_{60}	$ZnP^{\bullet+}$−$C_{60}^{\bullet-}$	benzonitrile	9.4×10^8
H_2P−C_{60}	*H_2P−C_{60}	toluene	1.1×10^9
ZnP−H_2P	ZnP−*H_2P	benzonitrile	1.08×10^9
ZnP−H_2P	ZnP−*H_2P	toluene	9.1×10^8
ZnP−H_2P−C_{60}	ZnP−*H_2P− C_{60}	toluene	9.2×10^8
ZnP−H_2P−C_{60}	$ZnP^{\bullet+}$−H_2P−$C_{60}^{\bullet-}$	benzonitrile	4.6×10^7

^{3}*($\pi-\pi$*)H_2P, respectively, were measured in the present study (Table 3). Analogous to previous studies we ascribe the intermolecular reaction to the following photosenitization process of cytotoxic singlet oxygen:[50,51]

$$^3\text{*ZnP} + O_2 \rightarrow \text{ZnP} + {}^1\text{*}O_2 \qquad (2a)$$

$$^3\text{*}H_2\text{P} + O_2 \rightarrow H_2\text{P} + {}^1\text{*}O_2 \qquad (2b)$$

C_{60}−Ar. The photophysics of the fullerene reference (**C_{60}−Ar**, see Figure 2) can be summarized as follows: The singlet excited-state absorption of **C_{60}−Ar** gives rise to a marked singlet−singlet absorption around 890 nm, whose lowest vibronic state has an energy of 1.75 eV. The latter was determined in a complementary fluorescence measurement. Once generated, this state is subject to a rapid and quantitative intersystem crossing process to the energetically lower-lying triplet excited state (1.50 eV).[27] In the case of the currently employed fullerene reference (**C_{60}−Ar**), this intersystem crossing takes place with a time constant of 5.5×10^8 s^{-1}, governed by a large spin−orbit coupling.[52] The spin−orbit coupling makes this process much faster than those noticed in most 2-dimensional aromatic hydrocarbons. However, not only is the rate remarkable, but also the overall efficiency of this process is impressive, affording a triplet quantum yield close to unity ($\Phi_{TRIPLET} = 0.98$).[52] The triplet−triplet absorption spectrum reveals a maximum in the visible region (700 nm), accompanied by another transition in the ultraviolet (UV) region (360 nm). The triplet lifetime of **C_{60}−Ar** is dominated by triplet−triplet annihilation and ground-state quenching and is quite short, ~25 μs, under our standard conditions. It should be added that these features are consistent with the general trend noticed for various mono-functionalized fullerene derivatives.[27]

$$\mathbf{C_{60}-Ar} \xrightarrow{h\nu} {}^1\text{*}\mathbf{C_{60}-Ar} \rightarrow {}^3\text{*}\mathbf{C_{60}-Ar} \qquad (3)$$

In summary, the above features (i.e., of reference compounds **ZnP**, **H_2P**, and **C_{60}−Ar**) are easily detectable markers for the following intramolecular transfer reactions. It is expected that the use of these probes will lead to a better understanding of functionalized fullerene and porphyrin derivatives and, in addition, that they will serve as a data set for the covalently linked, fullerene-containing porphyrin dyads and triad.

ZnP−H_2P. Transient absorption changes, recorded upon 532 nm laser excitation of the **ZnP−H_2P** dyad, are almost superimposable with those recorded for the ^{1}*($\pi-\pi$*)H_2P. Specifically, a set of minima, which correspond to the *Q*-band absorption (in toluene: 520, 556, 597, and 650 nm), is further accompanied by a new transient absorbing between 660 and 730 nm (Figure 4). Time profiles, taken at various wavelengths, indicate, however, that the singlet excited state (i.e., ^{1}*($\pi-\pi$*)H_2P) is formed in two distinct steps. The faster process lies essentially within the apparatus resolution (20 ps), while the second, slower component has a rise time of 79 ps (1.3×10^{10} s^{-1}) in toluene and 85 ps (1.2×10^{10} s^{-1}) in benzonitrile.

Complementary time-resolved fluorescence measurements of the **ZnP−H_2P** dyad revealed dual fluorescence. In particular, a rapid deactivation of the ^{1}*($\pi-\pi$*)ZnP fluorescence (605 nm) with an associated rate constant of 2.2×10^{10} s^{-1}, resembling the kinetics of the transient absorption measurements. On the other hand, the ^{1}*($\pi-\pi$*)H_2P fluorescence (720 nm) shows no indication for a faster decay.[46]

It is interesting to note that the absorption ratio at 695 nm, stemming from the faster (Figure 4, 25 ps time delay) and the slower process (Figure, 150 ps time delay), is approximately 1:1. This is in line with the nearly identical singlet ground-state absorption of the ZnP and H_2P moieties in **ZnP−H_2P** at the excitation wavelength (532 nm). Also, the weak absorption features of the initially formed ^{1}*($\pi-\pi$*)ZnP should be noted. Accordingly, it is safe to ascribe the secondary contribution to originate from an intramolecular singlet−singlet energy transfer between the ^{1}*($\pi-\pi$*)ZnP (2.04 eV) and the energetically lower-ying ^{1}*($\pi-\pi$*)H_2P (1.89 eV). A similar conclusion was reached from the time-resolved fluorescence measurements.[46]

$$\text{ZnP}-H_2\text{P} \xrightarrow{h\nu} {}^1\text{*ZnP}-H_2\text{P} \rightarrow \text{ZnP}-{}^1\text{*}H_2\text{P} \qquad (4)$$

According to the Coulombic energy transfer theory a singlet−singlet energy transfer is proportional to the square of the transition dipole moments and the inverse sixth power of the donor−acceptor separation (R_{D-A}). The distance dependence of this dipole−dipole mechanism can be simplified as follows considering the deactivation of the photoexcited chromophore (i.e., ^{1}*($\pi-\pi$*)ZnP; $k_D = 4.0 \times 10^8$ s^{-1}).[53]

$$\ln(k_{EnergyTransfer}/k_D) \approx 6 \ln(R_{D-A}) \qquad (5)$$

At the given donor−acceptor separation of 18 Å, the rapid and efficient energy transfer from the ^{1}*($\pi-\pi$*)ZnP to the H_2P is in agreement from the Coulombic energy-transfer theory,

(52) Foote, C. S. *Top. Curr. Chem.* **1994**, *169*, 347.

(53) Turro, N. J. *Modern Molecular Photochemistry*; University Science Books, Sausalito, CA, 1978.

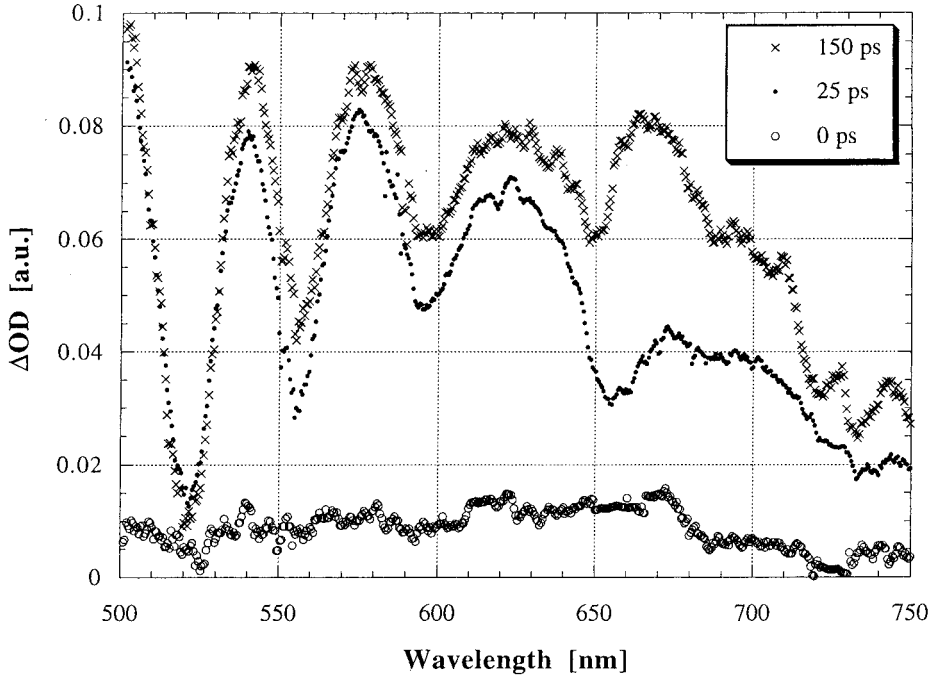

Figure 4. Differential absorption spectra obtained upon picosecond flash photolysis (532 nm) of $\sim 10^{-5}$ M solutions of **ZnP−H$_2$P** dyad in nitrogen saturated toluene with a time delay of 0 ps (○), 25 ps (•), and 150 ps (×).

which, in its essence, predicts that the dipole−dipole mechanism is mostly effective up to separations of ~20 Å.

Complementary nanosecond experiments, performed with a similar **ZnP−H$_2$P** dyad solution, revealed a maximum at 780 nm (see Figure 3 c) and a lifetime of 380 μs. These are again unambiguous attributes of the ^{3}*($\pi-\pi$*)H$_2$P. The overall triplet quantum yields, as measured with the comparative method (i.e., using **H$_2$P** as a standard), are 0.76 (toluene) and 0.74 (benzonitrile), are slightly lower than the one found for the **H$_2$P** reference compound ($\Phi_{TRIPLET} = 0.82$). These properties confirm our tentative assignment of a singlet−singlet energy-transfer mechanism controlling the deactivation of the photoexcited ZnP in the **ZnP−H$_2$P** dyad.

Similar to the reference compound (see eq 2b), admitting molecular oxygen to the dyad solution led to a rapid deactivation of the ^{3}*($\pi-\pi$*)H$_2$P state with bimolecular rate constants of 9.1×10^8 M^{-1} s^{-1} and 1.08×10^9 M^{-1} s^{-1} in toluene and benzonitrile, respectively (see Table 3). It should be added that singlet oxygen is the product of this bimolecular reaction.[54] In conclusion, the spatially separated **ZnP−H$_2$P** is subject, upon excitation of the ZnP chromophore, to an efficient long-range intramolecular energy transfer. Similar conclusions stem from previous reports on chemically different ZnP−H$_2$P dyads.[55]

In the contributed system, the free-energy changes ($-\Delta G_{CS}$) for an intramolecular electron-transfer event is −0.61 eV in toluene and 0.15 eV in benzonitrile. Only electron-donating and electron-withdrawing substituents at the ZnP and H$_2$P, respectively, render the free-energy change for an intramolecular electron transfer thermodynamically more feasible, yielding a ZnP$^{\bullet+}$−H$_2$P$^{\bullet-}$ radical pair.[55]

ZnP−C$_{60}$. The two porphyrin−fullerene dyads, **ZnP−C$_{60}$** and **H$_2$P−C$_{60}$**, are expected to undergo intramolecular electron transfer, as shown earlier in porphyrin−fullerene dyads that carried different linking blocks.[38−45] This assumption is, furthermore, supported by calculations regarding the thermodynamic driving force ($-\Delta G_{CS}$) within the framework of the dielectric continuum model (see Table 1).[47,48] However, in the event that nonpolar toluene is used as a solvent, the efficiency of electron transfer versus the competing energy transfer will depend strongly on the separation distance and may alter the mechanism. Considering the distance dependence on electron transfer (eq 6 with $k_D = 4.0 \times 10^8$ s^{-1})[53] we can expect that at short donor−acceptor separations (~3 Å) electron-transfer prevails.[45b] L is the electronic factor, characterizing the overlap of orbitals involved in the electron-transfer reactions.[53] At larger spatial separations, such as in the current dyads and triad (18 Å), it is likely that energy transfer is the dominant process.

$$\ln(k_{\text{Electron Transfer}}/k_D) \approx 2R_{D-A}/L \qquad (6)$$

Following a 18 ps laser pulse of a benzonitrile solution of the **ZnP−C$_{60}$** dyad, differential absorption changes disclose the instaneous formation of the ZnP singlet excited state (Figure 5, 30 ps). The two minima observed at 565 and 605 nm correspond well to the slightly shifted *Q*-band absorption, due to the complexation of the coordinating solvent (e.g., benzonitrile).[45a,d] These features, in combination with the broad absorption band in the red (>620 nm) demonstrate the excitation of the ZnP. The lifetime of the ^{1}*($\pi-\pi$*)ZnP is, however, impacted by the presence of the covalently attached electron acceptor (i.e., fullerene). Formation of a new transient develops as a result of the rapid decay ($k = 1.1 \times 10^{10}$ s^{-1}), instead of the much slower intersystem crossing (4.0×10^8 s^{-1}) to the triplet excited state.

(54) Röder, B. *Biophys. Chem.* **1990**, *35*, 303.
(55) (a) Gust, D.; Moore, T. A.; Moore, A.; Leggett, L.; Lin, S.; DeGraziano, J. M.; Hermant, R. M.; Nicodem, D.; Craig, P.; Seely, G. R.; Nieman, R. A. *J. Phys. Chem.* **1993**, *97*, 7926. (b) DeGraziano, J. M.; Liddell, P. A.; Leggett, L.; Moore, A.; Moore, T. A.; Gust, D. *J. Phys. Chem.* **1994**, *98*, 1758. (c) Yang, S. I.; Lammi, R. K.; Seth, J.; Riggs, J. A.; Arai, T.; Kim, D.; Bocian, D. F.; Holten, D.; Lindsey, J. S. *J. Phys. Chem. B* **1998**, *102*, 9426. (d) Baraka, M. E.; Jano, J. M.; Ruhlmann, L.; Giraudeau, A. Deumie, M.; Seta, P. *J. Photochem. Photobiol. A* **1998**, *113*, 163. (e) Jensen, K. K.; Van Berlkom, S. B.; Kajanus, J.; Martensson, J.; Albinsson, B. *J. Phys. Chem. A* **1997**, *101*, 2218. (f) Osuka, A.; Marumo, S.; Mataga, N.; Taniguchi, S.; Okada, T.; Yamazaki, I.; Nishimura, Y.; Ohno, T.; Nozaki, K. *J. Am. Chem. Soc.* **1996**, *118*, 155. (g) Gust, D.; Moore, T. A.; Moore, A.; Kang, H. K.; DeGraziano, J. M.; Liddell, P. A.; Seely, G. R. *J. Phys. Chem.* **1993**, *97*, 13637. (h) Kilsa, K.; Kajanius, J.; Martensson, J.; Albinsson, B. *J. Phys. Chem. B* **1999**, *103*, 7329.

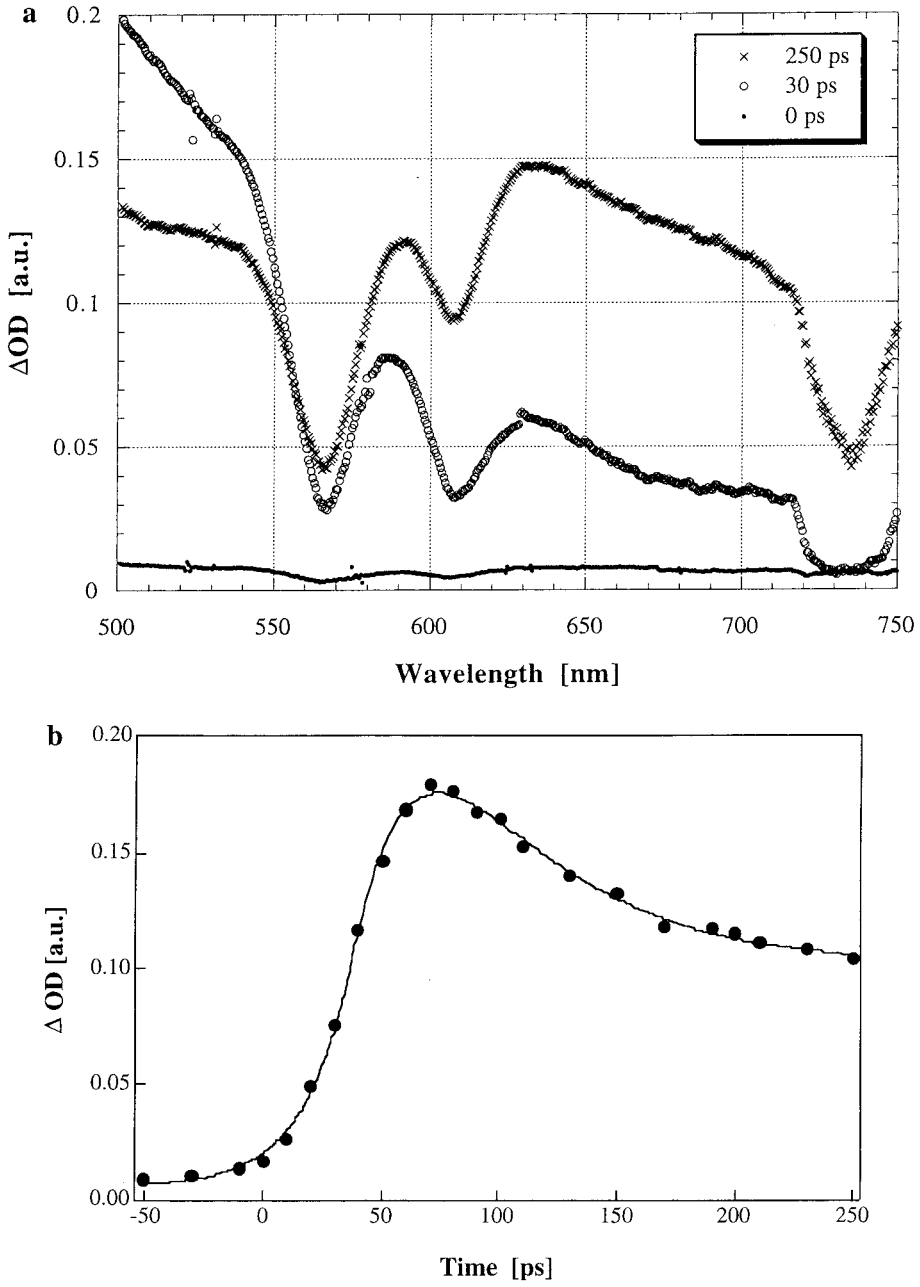

Figure 5. (a) Differential absorption spectra obtained upon picosecond flash photolysis (532 nm) of $\sim 10^{-5}$ M solutions of **ZnP**−**C$_{60}$** dyad in nitrogen saturated benzonitrile with a time delay of 0 ps (•), 30 ps (○), and 250 ps (×). (b) Time-absorption profile at 502 nm, displaying the initial formation of the ^{1}*(π−*π)ZnP chromophore and its subsequent transformation via an intramolecular electron transfer to the charge-separated radical pair (ZnP$^{\bullet+}$−C$_{60}^{\bullet-}$) (~250 ps after the pulse).

The new transient absorbs predominantly in a region red-shifted relative to the porphyrin *Q*-bands (Figure 5, 250 ps, see kinetic time trace).[44a,b] This suggests involvement of the ZnP π-radical cation in an intramolecular electron transfer, occurring between the photoexcited ZnP donor and the fullerene acceptor.

$$\text{ZnP}-\text{C}_{60} \xrightarrow{h\nu} {}^1\text{*ZnP}-\text{C}_{60} \rightarrow \text{ZnP}^{\bullet+}-\text{C}_{60}^{\bullet-} \qquad (7)$$

With the assistance of complementary nanosecond experiments (Figure 6) the presence of the one-electron-reduced fullerene, exhibiting a characteristic absorption maximum at 1000 nm, was also confirmed.[56,57] These experiments (i.e., measurements at 1000 nm) enabled us, furthermore, to determine the lifetime of the charge-separated ZnP$^{\bullet+}$−C$_{60}^{\bullet-}$ pair ($\tau = 580$ ns) and the quantum yield as well ($\Phi = 0.85$) in deoxygenated benzonitrile solutions.

It is notable that molecular oxygen has a meaningful impact on the lifetime of the charge-separated state. Reoxidation of the fullerene π-radical anion and, in turn, the possible formation of $O_2^{\bullet-}$ may take place.[58,59] This assumption is reasonable considering our measured redox potential for the first reduction step of the fullerene moiety ($E_{1/2}$ (C$_{60}$/C$_{60}^{\bullet-}$) = −1.04 V vs Fc/Fc$^+$) and $E_{1/2}$ for the $O_2/O_2^{\bullet-}$couple (−0.9 V vs Fc/Fc$^+$). In particular, we derived from an oxygen-dependent decay of the fullerene π-radical anion absorption an intermolecular rate

(56) Guldi, D. M.; Hungerbuehler, H.; Janata, E.; Asmus, K. D. *J. Chem. Soc., Chem. Commun.* **1993**, *6*, 84.
(57) Kato, T.; Kodama, T.; Shida, T.; Nakagawa, T.; Matsui, Y.; Suzuki, S.; Shiromaru, H.; Yamauchi, K.; Achiba, Y. *Chem. Phys. Lett.* **1991**, *180*, 446.
(58) Ohlendorf, V.; Willnow, A.; Hungerbuhler, H.; Guldi, D. M.; Asmus, K.-D. *J. Chem. Soc., Chem. Commun.* **1995**, 759.
(59) Yamakoshi, Y.; Sueyoshi, S.; Fukuhara, K.; Miyata, N.; Masumizu, T.; Kohno, M. *J. Am. Chem. Soc.* **1998**, *120*, 12363.

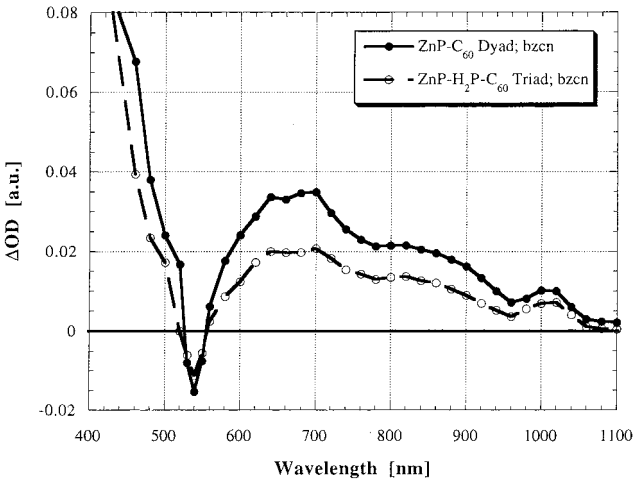

Figure 6. Differential absorption spectra obtained 50 ns upon nanosecond flash photolysis (532 nm) of ~10^{-5} M solutions of **ZnP−C$_{60}$** dyad in nitrogen saturated benzonitrile (—) and **ZnP−H$_2$P−C$_{60}$** triad in nitrogen saturated benzonitrile (— — —).

constant of 9.4×10^8 M^{-1} s^{-1}. This value is close to a diffusion-controlled process (i.e., $k_{diff} = 5.0 \times 10^9$ M^{-1} s^{-1}) as computed from Smoluchowski's theory of diffusion-controlled reactions (with $k_{diff} = 8RT/3\eta \times 10^3$; $\eta_{(benzonitrile)} = 1.24$ [10^{-3} Pa × s]).[49]

$$ZnP^{\bullet+}-C_{60}^{\bullet-} + O_2 \rightarrow ZnP^{\bullet+}-C_{60} + O_2^{\bullet-} \qquad (8)$$

In toluene, two distinct follow-up reactions come next after the completion of the initially formed ^{1}*($\pi-\pi$*)ZnP state. The first process is a fast decay, which is essentially completed around 100 ps after the laser pulse with a rate constant of 1.7×10^{10} s^{-1} (see 500−550 nm region). In contrast, the second, slower step is a growing-in process with a time constant of 1.8 ns ($k = 5.5 \times 10^8$ s^{-1}) (see 650−750 nm region). This observation is in clear contrast to the benzonitrile case that revealed only a rapidly occurring electron transfer. Spectral analysis of the two transients formed in toluene, for example, after 100 and 4000 ps (Figure 7), shows surprisingly no resemblance with the ZnP π-radical cation absorption (see Figure 5, 250 ps). Instead, the earlier formed species has a broad and structureless transition in the 550−750 nm range (Figure 7, 100 ps). These characteristics are similar to those noted for the fullerene singlet excited-state absorption.[27,60] The slower produced transient (Figure 7, 4000 ps) possesses the characteristics of the fullerene triplet excited state, for example, a maximum at 700 nm. Consequently, we reach the conclusion that a long-range singlet−singlet energy transfer, by means of a dipole−dipole mechanism (see eq 5) governs the deactivation of the photoexcited ZnP.

Also, the thermodynamic argument (see Table 1), that is, the calculated driving force ($-\Delta G_{CS}$), contradicts an electron-transfer event in toluene. Although $-\Delta G_{CS}$ is clearly smaller (−0.13 eV), relative to the benzonitrile case (+0.69 eV), the decay of the ^{1}*($\pi-\pi$*)ZnP component is evidently faster in toluene. The large $-\Delta G_{CS}$ value relates primarily to the lowering of the energy of the charge-separated state in the polar solvent and the stabilization resulting therefrom. In summary, the energetics and the observed rate indicate an energy transfer process in toluene.

To follow up on this argument and to investigate the presumed singlet−singlet energy transfer, we probed the growing-in of the fullerene singlet excited state and related it to the deactivation of the photoexcited ZnP chromophore. This measurement is possible because the absorption of the ^{1}*($\pi-\pi$*)ZnP is weak in the wavelength region where the predominant ^{1}*C$_{60}$ absorption is located (around 890 nm).[27,60] Indeed, the **ZnP−C$_{60}$** dyad shows, upon laser irradiation in toluene, the growing-in of the fullerene singlet excited state absorption. More importantly the formation kinetics of the fullerene singlet (1.7×10^{10} s^{-1}) were virtually identical to those of the decay of the ^{1}*($\pi-\pi$*)ZnP absorption around 500−650 nm (1.6×10^{10} s^{-1}).

$$ZnP-C_{60} \xrightarrow{h\nu} {}^1*ZnP-C_{60} \rightarrow ZnP-{}^1*C_{60} \rightarrow ZnP-{}^3*C_{60} \qquad (9)$$

In line with this energy-transfer mechanism, the differential absorption changes, recorded immediately after a 20 ns pulse, showed the spectral features of the fullerene triplet excited state. Specifically, two maxima located at 360 and 700 nm and a low-energy shoulder around 800 nm were observed.[27,60,61a] Also the high quantum yield of the fullerene triplet ($\Phi_{TRIPLET} = 0.86$) should be noted. Our analysis clearly shows the photosensitization effect of the porphyrin antenna. This enables the efficient fullerene triplet generation, even in a wavelength region where the fullerene absorption is relatively weak ($\epsilon_{532\ nm} \approx 2000$ M^{-1} cm^{-1}). No spectral evidence, in terms of the fullerene π-radical anion absorption at 1000 nm,[56,57] was observed that would be in support of a possible electron-transfer mechanism.

H$_2$P−C$_{60}$. In benzonitrile solutions, the singlet−singlet absorption of the ^{1}*($\pi-\pi$*)H$_2$P, formed directly upon photolysis, decays rapidly. The derived rate constant of 5.2×10^9 s^{-1} is in sharp contrast to the much slower occurring intersystem crossing rate (9.9×10^7 s^{-1}), observed for the reference **H$_2$P** complex (see Tables 2 and 4). The spectral features of the newly formed transient, that is, a broad band red-shifted with regard to the *Q*-band absorption, are similar to the radiolytically formed π-radical cation of the H$_2$P (not shown). This suggests a rapid intramolecular electron transfer to yield the $H_2P^{\bullet+}-C_{60}^{\bullet-}$ state. The lower singlet excited-state energy (1.89 eV) and, in addition, the less favorable oxidation potential ($E_{1/2}$ ($H_2P^{\bullet+}/H_2P$) = +0.55 V vs Fc/Fc^+) of the free base porphyrin, relative to the ZnP dyad ($E_{1/2}$ ($ZnP^{\bullet+}/ZnP$) = +0.34 V vs Fc/Fc^+), have a marked impact on the electron-transfer dynamics. Despite the identical separation, for example, a center-to-center distance of 18.0 Å, $-\Delta G_{CS}$ for an electron transfer is only +0.33 eV (**H$_2$P−C$_{60}$**), in comparison to a value of +0.69 eV for the **ZnP−C$_{60}$** dyad (see Table 1).

Full spectral characterization of the charge-separated state was performed with the help of complementary nanosecond measurements. Photolysis of a similar **H$_2$P−C$_{60}$** solution led to a maximum at 1000 nm, which is a clear indication for the existence of the fullerene π-radical anion.[56,57] This $C_{60}^{\bullet-}$ fingerprint allowed us to determine the lifetime of the associated charge-separated state to be ~45 ns. The latter decays via another intermediate to the ^{3}*($\pi-\pi$*)H$_2$P, characterized by a transition maximizing around 780 nm (similar to Figure 3, spectrum a). The 780 nm band resembles those recorded for the **H$_2$P** and **ZnP−H$_2$P** references. In deoxygenated solutions

(60) Guldi, D. M.; Maggini, M.; Scorrano G.; Prato, M. *J. Am. Chem. Soc*. **1997**, *119*, 974.

(61) (a) Guldi, D. M.; Maggini, M. *Gazz. Chim. Ital*. **1997**, *127*, 779. (b) Martin, N.; Sanchez, L.; Illescas, B.; Gonzalez, S.; Herranz, M. A.; Guldi, D. M. *Carbon* **2000**, in press. (c) Guldi, D. M.; Gonzalez, S.; Martin, N.; Anton, A.; Garin, J.; Orduna, J. *J. Org. Chem.* **2000**, *65*, 1978−1983..

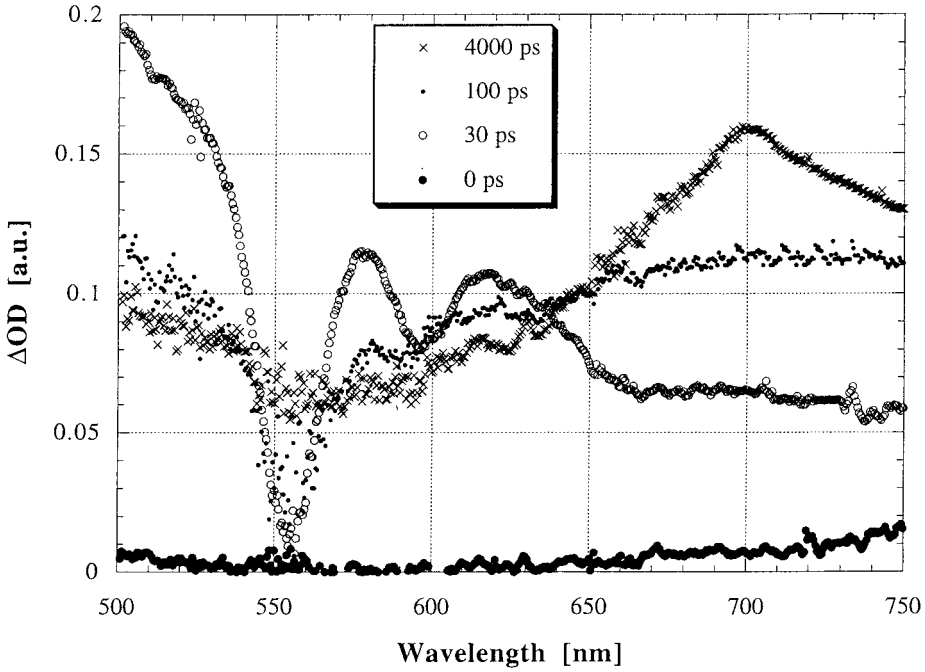

Figure 7. Differential absorption spectra obtained upon picosecond flash photolysis (532 nm) of $\sim 10^{-5}$ M solutions of **ZnP−C$_{60}$** dyad in nitrogen saturated toluene with a time delay of 0 ps (●), 30 ps (○), 100 ps (•), and 4000 ps (×).

Table 4. Center-to-center Distances and Rate Constant for Intramolecular Electron Transfer in Fullerene−Porphyrin Dyads and Triad

compd	solvent	R_{D-A} [Å]	k_{ET} [s^{-1}]	k_{BET} [s^{-1}]
H$_2$P$^{\bullet+}$−C$_{60}^{\bullet-}$	benzonitrile	18.0	5.2×10^9	1.3×10^7
ZnP$^{\bullet+}$−C$_{60}^{\bullet-}$	benzonitrile	18.0	1.1×10^{10}	1.3×10^6
ZnP−H$_2$P$^{\bullet+}$−C$_{60}^{\bullet-}$	benzonitrile	18.0	7.0×10^9	
ZnP$^{\bullet+}$−H$_2$P−C$_{60}^{\bullet-}$	benzonitrile	36.1	2.2×10^9	4.7×10^4

the ^{3}*($\pi-\pi$*)H$_2$P gives rise to a lifetime of 231 μs, decaying to the singlet ground state. At this point we cannot offer any reasonable rationale for the nature of the transient intermediate. However, a similar ET behavior was reported in a C−C$_{60}$ dyad (C = carotenoid polyene),[38g] C−H$_2$P−C$_{60}$ triad,[38d] and tetrathiafulvalene−C$_{60}$ dyad[61b,61c] where BET proceeds mainly via formation of the carotenoid triplet excited state (C−C$_{60}$ and C−H$_2$P−C$_{60}$)[38d,g] and fullerene triplet excited state (tetrathiafulvalene-C$_{60}$).[61b,c]

In toluene solutions the decay of the ^{1}*($\pi-\pi$*)H$_2$P moiety of **H$_2$P−C$_{60}$** is subject to a similar change in mechanism as described above for the **ZnP−C$_{60}$** dyad. Specifically, a rapid singlet−singlet energy transfer (1.5×10^{10} s^{-1}) takes place to yield the fullerene singlet excited state. This is followed by an intersystem crossing (5.6×10^8 s^{-1}) to the energetically lower-lying fullerene triplet (similar to Figure 7). In the **ZnP−C$_{60}$** dyad the fullerene triplet excited state (i.e., ZnP−^{3}*C$_{60}$) is lowest state available and, in turn, decayed to the singlet ground state. Now, in the case of the current **H$_2$P−C$_{60}$** dyad, the energy of the ^{3}*($\pi-\pi$*)H$_2$P state (1.40 eV), is located between the fullerene triplet (1.50 eV) and the singlet ground state. As a consequence, an additional, but rather slow ($k = 2.4 \times 10^5$ s^{-1}) triplet−triplet energy transfer from the fullerene triplet to the porphyrin is energetically permitted. Considering the center-to-center distance of 18.0 Å, the much slower rate constant, relative to the singlet−singlet energy transfer ($\sim 10^{10}$ s^{-1}), can be rationalized by the different mechanisms, namely, dipole−dipole (see eq 5) versus exchange (see eq 6), which are operative in this system.[53] In addition, the triplet quantum yields further underlines the noted differences. While the intermediately generated fullerene triplet excited state (e.g., H$_2$P−^{3}*C$_{60}$) gives rise to an overall efficiency of 83%, only a moderate 54% were determined for the final product (e.g., ^{3}*H$_2$P−C$_{60}$).

$$H_2P-C_{60} \xrightarrow{h\nu} {}^1{*}H_2P-C_{60} \rightarrow H_2P-{}^1{*}C_{60} \rightarrow H_2P-{}^3{*}C_{60} \rightarrow {}^3{*}H_2P-C_{60} \quad (10)$$

ZnP−H$_2$P−C$_{60}$. Stimulated by the above findings, we pursued the design of a molecular array, in which the free base porphyrin separates the zinc porphyrin from the electron acceptor. This strategy should, in principle, allow a charge shift from the one-electron oxidized H$_2$P π-radical cation ($E_{1/2}$ (H$_2$P$^{\bullet+}$/H$_2$P) = +0.59 V vs Fc/Fc$^+$) to the better electron donor ZnP ($E_{1/2}$ (ZnP$^{\bullet+}$/ZnP) = +0.30 V vs Fc/Fc$^+$), prior to the charge-recombination of the initially formed ZnP−H$_2$P$^{\bullet+}$−C$_{60}^{\bullet-}$.

Benzonitrile. The whole dynamic range (e.g., between −50 and 4000 ps), in terms of differential absorption changes, recorded upon 532 nm excitation of a **ZnP−H$_2$P−C$_{60}$** benzonitrile solution, is depicted in Figure 8. The initial events are virtually identical to those described above for the diporphyrin reference dyad (**ZnP−H$_2$P**): Two successive steps are associated with the formation of the ^{1}*($\pi-\pi$*)H$_2$P, which then may inject an electron into the fullerene moiety. These are (i) direct 532 nm excitation of the H$_2$P chromophore and (ii) rapid intramolecular singlet−singlet energy transfer ($k = 1.5 \times 10^{10}$ s^{-1}) originating from the ^{1}*($\pi-\pi$*)ZnP (Figure 9). Importantly, the measured energy transfer rate closely resembles the dynamics of the **ZnP−H$_2$P** dyad (see above) and the time-resolved fluorescence measurements.[46]

An interesting fact is that even in the case of the molecular triad, the ratio of the direct excitation and the energy transfer is nearly 1:1 as measured by the growing-in of the transient around 695 nm (see also the discussion regarding the energy transfer in the photoexcited **ZnP−H$_2$P** dyad). This is in compliance with the nearly equal absorbance of the two chromophores (i.e., ZnP and H$_2$P) at the excitation wavelength (532 nm).

The initial excitation energy is almost quantitatively ($\sim$75%, see **ZnP−H$_2$P**) transferred to the H$_2$P chromophore. After the

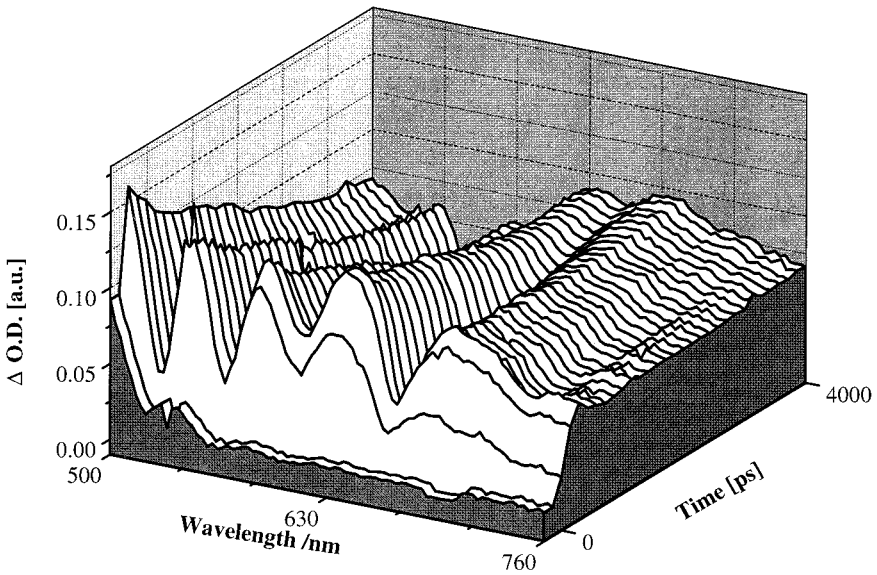

Figure 8. Differential absorption spectra obtained upon picosecond flash photolysis (532 nm) of ~10^{-5} M solutions of **ZnP−H$_2$P−C$_{60}$** triad in nitrogen saturated benzonitrile with time delays of between −50 and 4000 ps.

completion of this energy transfer process, the sequence of two follow-up reactions was noticed (see kinetic time trace of Figure 10). The faster one has a time constant of 7.0×10^9 s^{-1} (see Table 4). Based on the kinetic similarity with the electron transfer in the **H$_2$P−C$_{60}$** dyad, we ascribe this reaction tentatively to the formation of the $H_2P^{\bullet+}-C_{60}^{\bullet-}$ pair in the molecular triad. Spectral characteristics of the porphyrin π-radical cation, particularly, in the red region, corroborated this hypothesis (Figure 10, 500 ps).

The energy of the $ZnP-H_2P^{\bullet+}-C_{60}^{\bullet-}$ state (1.60 eV) lies sufficiently above that of the long-range separated pair, namely, $ZnP^{\bullet+}-H_2P-C_{60}^{\bullet-}$ (1.32 eV). In principle the noted energy difference should be enough to promote a subsequent charge shift from the $H_2P^{\bullet+}$ to the ZnP. Indeed, the spectral features, recorded 3000 ps after the pulse (Figure 10, 3000 ps), are reminiscent to the charge-separated state in the **ZnP−C$_{60}$** reference dyad and, therefore, support the energetics argument. From the growing-in kinetics of the ZnP π-radical cation at 650 nm we were able to derive a rate constant for this secondary electron transfer of 2.2×10^9 s^{-1}.

Complementary nanosecond experiments revealed the spectral features of both radical species, namely, the oxidized $ZnP^{\bullet+}$ (600−750 nm) and the reduced $C_{60}^{\bullet-}$ (1000 nm) (Figure 6). The long-range charge-separated pair is formed with a quantum yield of 0.4. Due to the large spatial separation of 36.1 Å the $ZnP^{\bullet+}-H_2P-C_{60}^{\bullet-}$ decays with a remarkable lifetime of 21 μs. The charge recombination process is dominated by a monoexponential recovery of the singlet ground-state rather than population of a porphyrin triplet excited state. This observation corresponds well with the energetic argument (1.32 eV).

532 nm (benzonitrile):

$$ZnP-H_2P-C_{60} \xrightarrow{-h\nu} {}^1{*}ZnP-H_2P-C_{60} \rightarrow ZnP\text{-}{}^1{*}H_2P-C_{60} \rightarrow ZnP-H_2P^{\bullet+}-C_{60}^{\bullet-} \rightarrow ZnP^{\bullet+}-H_2P-C_{60}^{\bullet-} \quad (11)$$

The lifetime of the $ZnP^{\bullet+}-H_2P-C_{60}^{\bullet-}$ radical pair, opened the opportunity for a reaction with molecular oxygen. Admission of air or pure oxygen to the triad solution resulted in a markedly accelerated recovery of the fullerene ground state. From analyzing the lifetime as a function of oxygen concentration an intermolecular rate constant of $k = 4.6 \times 10^7$ M^{-1} s^{-1} was derived. This leads to the conclusion that $C_{60}^{\bullet-}$ is quantitatively reoxidized by oxygen. Since the reduction potential of the fullerene moiety (−1.04 V vs Fc/Fc^+) is not changed relative the one in the **ZnP−C$_{60}$** dyad, the following reduction of molecular oxygen ($E_{1/2}$ ($O_2/O_2^{\bullet-}$) = −0.9 V vs Fc/Fc^+) appears thermodynamically reasonable:

$$ZnP^{\bullet+}-H_2P-C_{60}^{\bullet-} + O_2 \rightarrow ZnP^{\bullet+}-H_2P-C_{60} + O_2^{\bullet-} \quad (12)$$

Comparing the individually determined rate constants for (i) an intramolecular electron transfer in benzonitrile (7.0×10^9 s^{-1}) and (ii) an energy transfer in toluene (1.5×10^{10} s^{-1}, see below) leads to the hypothesis that in benzonitrile a competition between the two transfer processes is operative. A thermodynamic consideration ($-\Delta G_{CS} = 0.29$ eV; $-\Delta G_{EnergyTransfer} = 0.13$ eV) suggests, however, a minor contribution of the competing energy transfer mechanism. In good agreement with the thermodynamic reasoning, no spectral evidence for the participation of an energy transfer mechanism was deduced from our picosecond-resolved transient absorption measurements.

To shed further light on this alternative electron-transfer pathway, generation of the fullerene singlet excited state, which would be the result of the intramolecular energy transfer, was deemed necessary. An electron transfer starting from the photoexcited fullerene was probed via a 337 nm excitation experiment, where the fullerene moiety absorbs the main fraction of the excitation light. In fact, the transient absorptions, measured after a 20 ns laser pulse are essentially superimposable to those of the 532 nm excitation. In particular, features of the oxidized ZnP (600−750 nm) and the reduced fullerene moiety (1000 nm) confirm the following electron-transfer scenario:

337 nm (benzonitrile):

$$ZnP-H_2P-C_{60} \xrightarrow{-h\nu} ZnP-H_2P-{}^1{*}C_{60} \rightarrow ZnP-H_2P^{\bullet+}-C_{60}^{\bullet-} \rightarrow ZnP^{\bullet+}-H_2P-C_{60}^{\bullet-} \quad (13)$$

The determination of the quantum yield for the charge-separation showed surprisingly a higher value in the 337 nm than in the 532 nm experiment. This can be rationalized, at least in part, by the sequence of energy- and electron transfers

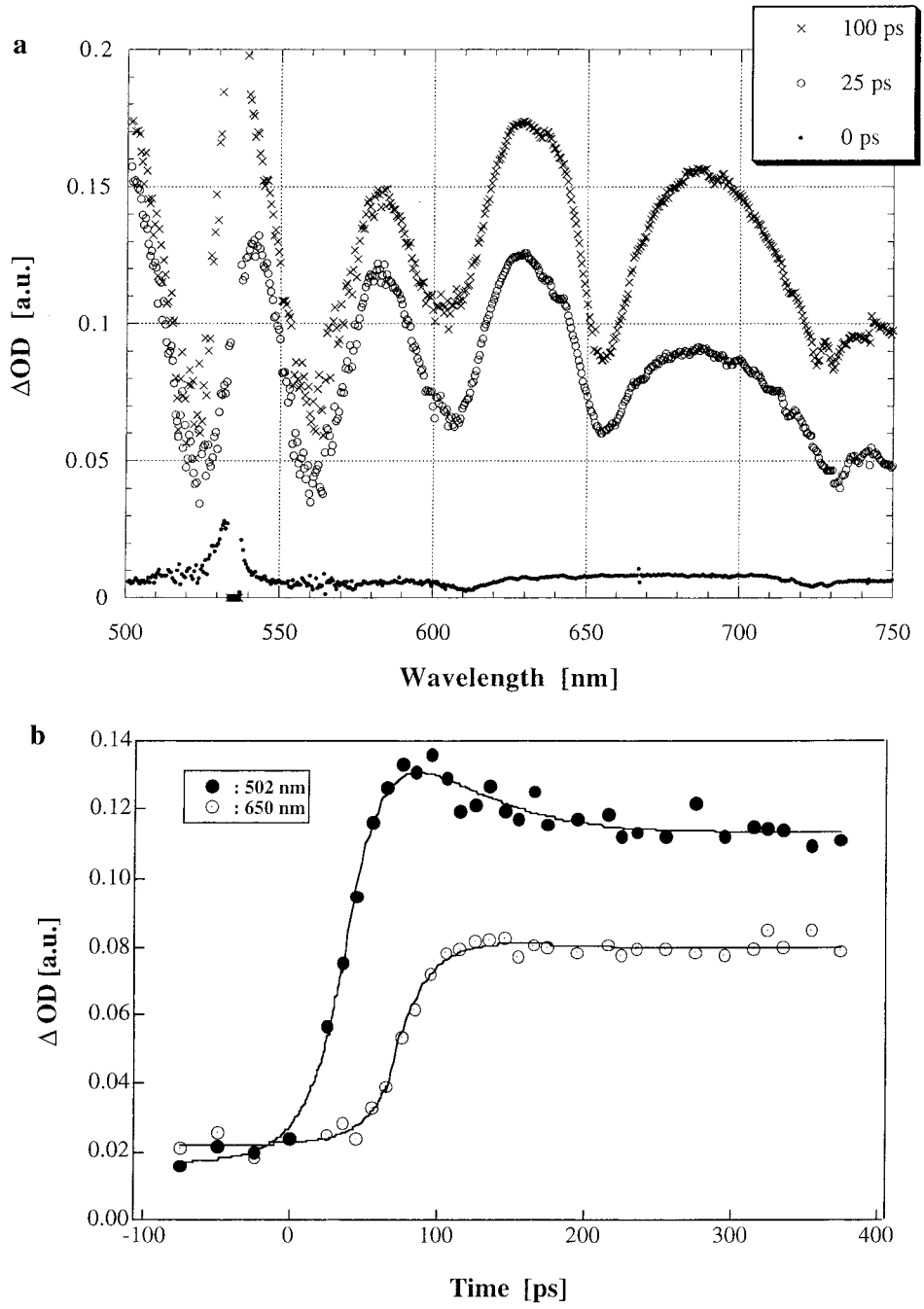

Figure 9. (a) Differential absorption spectra obtained upon picosecond flash photolysis (532 nm) of ~10^{-5} M solutions of **ZnP−H₂P−C₆₀** triad in nitrogen-saturated benzonitrile with a time delay of 0 ps (•), 25 ps (○), and 100 ps (×). (b) Time-absorption profiles at 502 and 650 nm, displaying the intramolecular energy transfer from the initially excited ^{1}*ZnP−H_2P−C_{60} to ZnP−^{1}*H_2P−C_{60}, (completed around 100 ps after the pulse) followed by an intramolecular electron-transfer yielding ZnP−$H_2P^{\bullet+}$−$C_{60}^{\bullet-}$ (~300 ps after the pulse).

involved upon excitation of the ZnP and H_2P chromophores in the **ZnP−H₂P−C₆₀** triad, which proceed with a quantum yield less than unity. On the other hand, excitation of the fullerene is nearly quantitative.

The conclusion of these experiments is that the formation of the charge-separated radical-pair (ZnP−$H_2P^{\bullet+}$−$C_{60}^{\bullet-}$ and consequently $ZnP^{\bullet+}$−H_2P−$C_{60}^{\bullet-}$) upon 532 nm excitation is independent of the pathway, namely, either direct electron transfer from the ^{1}*(π−π*)H_2P to the fullerene or, alternatively, energy transfer from the ^{1}*(π−π*)H_2P to the fullerene, followed by an electron transfer.[62]

Toluene. In nonpolar toluene the mechanism changed dramatically: The reactivity of the triad is now comparable to the sum of the two reference dyads in toluene, namely, energy transfer from ^{1}*(π−π*)ZnP to H_2P (**ZnP−H₂P**) and from ^{1}*(π−π*)H_2P to C_{60} (**H₂P−C₆₀**). The initial energy transfer event ($k = 1.5 \times 10^{10}$ s^{-1}) between the two porphyrin moieties was again confirmed by the two-step growing-in of the ^{1}*(π−π*)H_2P component around 695 nm (see above **ZnP−H₂P**).

(62) A similar consideration applies for the two precursor dyads (i.e., **H₂P−C₆₀** and **ZnP−C₆₀**). In nonpolar toluene rapid and efficient energy transfer governs the deactivation of the initially formed ^{1}*(π−π*)H_2P and ^{1}*(π−π*)ZnP states with rate constants of (1.5×10^{10} s^{-1}) and (1.7×10^{10} s^{-1}), respectively. An additional electron transfer starts, however, to compete with this energy transfer in polar benzonitrile. With the help of an 337 nm excitation experiments (e.g., fullerene excitation) it was confirmed that the ^{1}*C_{60} is potent enough to activate the intramolecular electron transfer from the fullerene end.

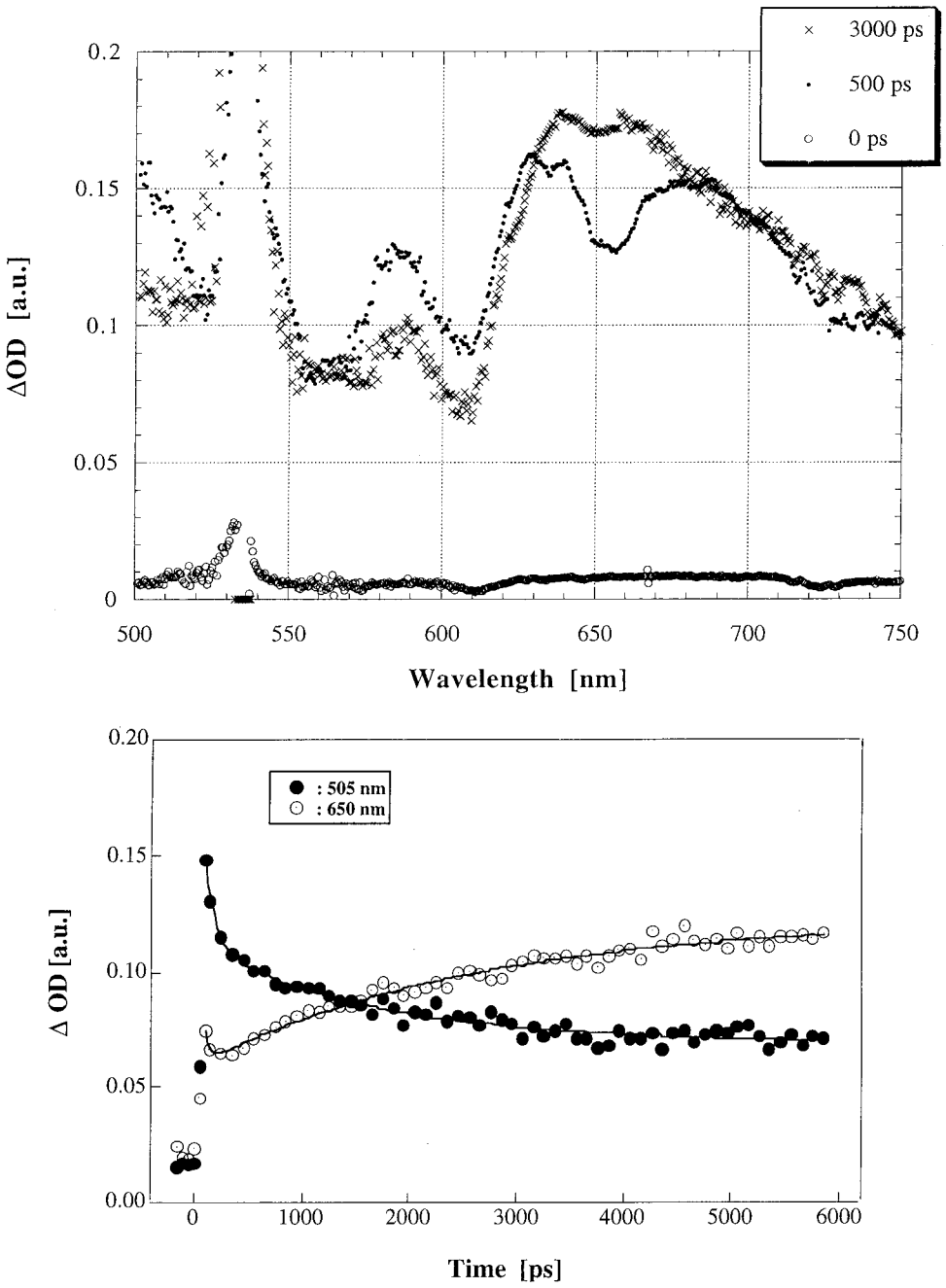

Figure 10. (a) Differential absorption spectra obtained upon picosecond flash photolysis (532 nm) of $\sim 10^{-5}$ M solutions of **ZnP−H$_2$P−C$_{60}$** triad in nitrogen saturated benzonitrile with a time delay of 0 ps (○), 500 ps (•), and 3000 ps (×). (b) Time-absorption profile at 505 and 650 nm (i.e., maximum difference between $H_2P^{\bullet+}$ and $ZnP^{\bullet+}$ absorption), displaying the charge-shift from the $ZnP-H_2P^{\bullet+}-C_{60}^{\bullet-}$ (~500 ps after the laser pulse) to $ZnP^{\bullet+}-H_2P-C_{60}^{\bullet-}$ (~5000 ps after the laser pulse).

Since the energy of the charge-separated $ZnP-H_2P^{\bullet+}-C_{60}^{\bullet-}$ is unfavorably raised in toluene (2.46 eV), relative to the benzonitrile solution (1.60 eV), energy transfer is expected to prevail over electron transfer. Indeed, singlet−singlet energy transfer from the $ZnP-{}^1{*}H_2P-C_{60}$ (1.90 eV) to the $ZnP-H_2P-{}^1{*}C_{60}$ (1.75 eV) governs the fate of the photoexcited chromophore.

532 nm (toluene):

$$ZnP-H_2P-C_{60} \xrightarrow{h\nu} {}^1{*}ZnP-H_2P-C_{60} \rightarrow ZnP-{}^1{*}H_2P-C_{60} \rightarrow ZnP-H_2P-{}^1{*}C_{60} \quad (14)$$

A direct energy-transfer route from the ZnP to the fullerene, over the estimated distance of 36.1 Å, should be comparable to the decay of the $^1{*}(\pi-\pi^*)$ZnP, according to the distance (R_{D-A}) dependence of the dipole−dipole mechanism (see eq 5).[53] Thus, the quantitative quenched ZnP fluorescence rules out the energetically feasible concerted long-range energy transfer instead of the stepwise transfer (i.e., from the ZnP to the H_2P and finally to the C_{60}). In fact, the experimental data disproves unequivocally the occurrence of a slow, concerted energy-transfer mechanism.

The fullerene singlet excited-state undergoes intersystem crossing to the triplet excited state, with a rate of 5.5×10^8 s^{-1} which was derived from the growing-in dynamics of the characteristic fullerene triplet excited-state absorption at 700 nm. Considering the fact that the intersystem crossing in fullerenes is near unity,[52] it is evident that the loss in efficiency

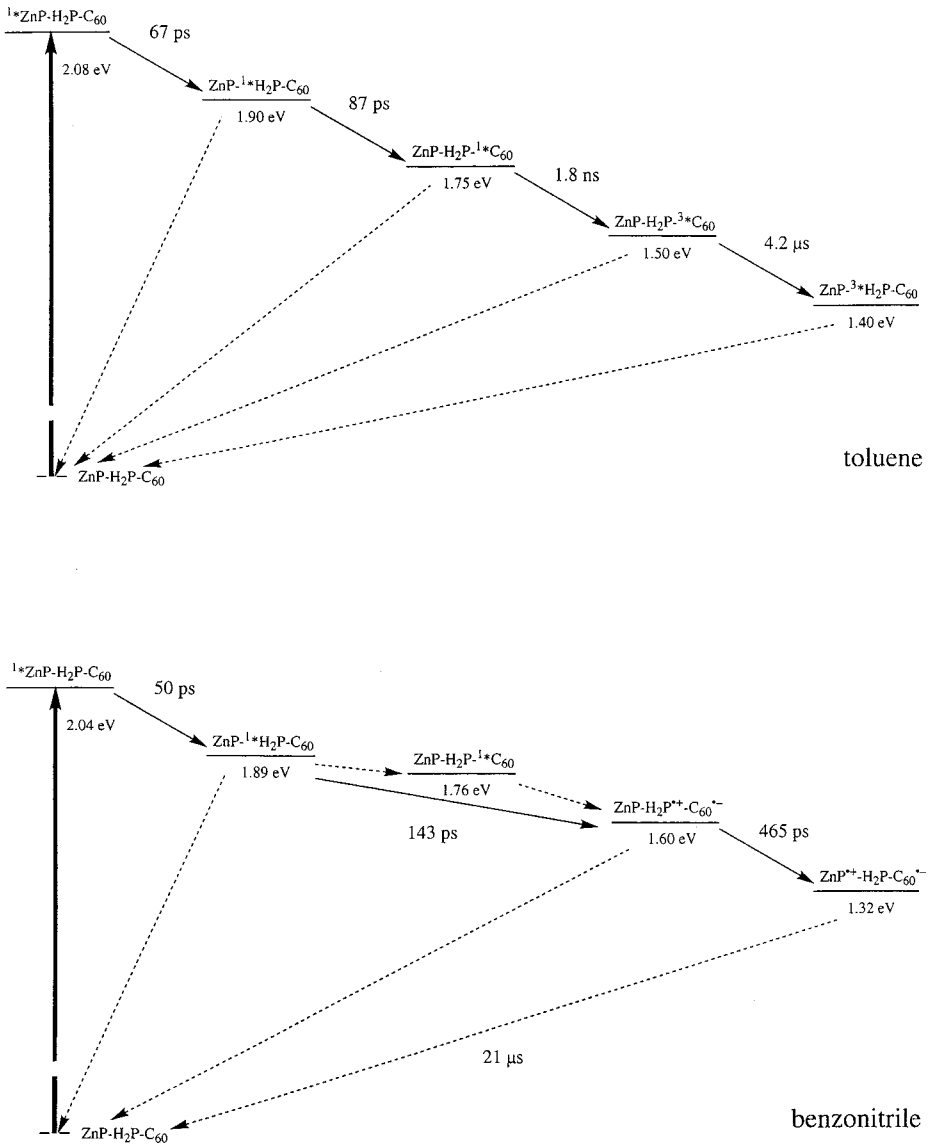

Figure 11. Energy diagram of **ZnP−H$_2$P−C$_{60}$** triad in toluene and benzonitrile.

(fullerene $\Phi_{TRIPLET} = 0.71$) corresponds well to the product, ^{1}*ZnP−H$_2$P−C$_{60}$/ZnP−^{1}*H$_2$P−C$_{60}$ ($\Phi = 0.92$) and ZnP−^{1}*H$_2$P−C$_{60}$/ZnP−H$_2$P−^{1}*C$_{60}$ ($\Phi = 0.83$) transformations. The fullerene triplet excited state decays finally via a slow and inefficient triplet−triplet energy transfer to the lowest lying state in the system (^{3}*($\pi-\pi$*)H$_2$P; 1.40 eV).

Conclusions

In conclusion, we demonstrated the sequential energy- and electron-transfer events in a supermolecular triad (lower part of the diagram in Figure 11) and, thus, a system that mimics the primary steps in natural photosynthesis. Furthermore, the lifetime of the charge-separated radical pair of 21 μs is promising and evokes further studies, for example, incorporation into heterogeneous systems.[63] It should be noted that the lifetime of the charge-separated radical pair, namely, ZnP$^{•+}$−H$_2$P−C$_{60}^{•-}$ implies a significant advancement not only with respect to C$_{60}$-based dyads but to C$_{60}$-based triads as well.[38−45] Considering the overall efficiency of 40% for (i) funneling light from the antenna chromophore (i.e., ZnP) to the H$_2$P chromophore, (ii) charge-injection into the fullerene core, and (iii) transportation of the hole, this artificial reaction center reproduces the natural system very well. Also its productiveness outperforms a recently published antenna−reaction center complex.[38f]

The higher efficiency of the current system, relative to previously investigated dyad and triad systems[38] cannot be explained on the basis of the thermodynamic redox properties of the species involved. One argument, which may, however, be forwarded, could be the fairly large separation existing between each of the redox active couples in **ZnP−C$_{60}$** (i.e., ZnP/C$_{60}$) and **ZnP−H$_2$P−C$_{60}$** (i.e., ZnP/H$_2$P and H$_2$P/C$_{60}$) of approximately 18 Å. In principle, this separation guarantees an efficient electron relay along the vertical energy gradient before, however, charge recombination takes over to dominate the fate of the first couple (i.e., ZnP−H$_2$P$^{•+}$−C$_{60}^{•-}$). A general comment, regarding the charge-injection from the photoexcited chromophore into the fullerene, should be made at this point. The small free energy change associated with the H$_2$P/C$_{60}$ couple, relative to that of the ZnP/C$_{60}$ couple is, at least, in part a major limitation of the system presented. Currently, we are pursuing work toward improving the initial charge-injection step.

In comparison to the previously published **ZnP−P34−C$_{60}$** dyad,[44b] the charge-separated ZnP$^{•+}$−C$_{60}^{•-}$ state even in **ZnP−**

(63) (a) Imahori, H.; Yamada, H.; Ozawa, S.; Ushida, K.; Sakata, Y. *Chem. Commun*. **1999**, 1165. (b) Imahori, H.; Yamada, H.; Nishimura, Y.; Yamazaki, I.; Sakata, Y. *J. Phys. Chem. B*, **2000**, *104*, 2099−2108.

C_{60} reveals a marked stabilization. Two structural differences in **ZnP−P34−C_{60}** vs **ZnP−C_{60}** are obvious. First, and far most important, the amide linkage, connecting the two redox-active centers is reversed. Second the different fullerene functionalization leads to the incorporation of additional C−C bond in **ZnP−C_{60}**. No doubt, the earlier reasoning appears to be of higher significance with regard to accelerating charge separation and to decelerating charge recombination.

On the other hand, in toluene solutions (upper part of the diagram in Figure 11) energy was transferred sequentially over a distance of 36.1 Å.

A different aspect of this study is concerned with the reactivity of the photoproducts (e.g., triplet excited states and charge-separated radical pairs) toward oxygen. All the triplet excited states generated (i.e., ^{3}*($\pi-\pi$*)H_2P, ^{3}*($\pi-\pi$*)ZnP and ^{3}*C_{60})[52,54,64,65] form singlet oxygen ($^1O_2$) with rate constants that are close to a diffusion controlled process and high efficiencies. Similarly, the two radical pairs formed (i.e., the short-lived $ZnP^{\bullet+}-C_{60}^{\bullet-}$ and the much longer lived $ZnP^{\bullet+}-H_2P-C_{60}^{\bullet-}$) are subject to a markedly slower reaction with molecular oxygen, yielding, however, the persistent superoxide radical anion ($O_2^{\bullet-}$).[58,59] Although the nature of the latter oxygen species differs from singlet oxygen, the product of the triplet excited-state quenching, its cytotoxicity should be considered. Thus, both reaction pathways, for example, energy- and electron transfer, result in reactive intermediates that, upon reaction with molecular oxygen, generate cytotoxic species.

Experimental Section

General. Melting points were determined on a Yanaco melting point apparatus and were uncorrected. IR spectra were obtained on a Perkin-Elmer System 2000 FT-IR. ^{1}H NMR spectra were measured on a JEOL JNM-EX270 or a JEOL JNM-LA400 using tetramethylsilane as internal standard. Fast atom bombardment mass (FABMS) and matrix-assisted laser desorption/ionization (MALDI) time-of-flight mass (TOFMS) spectra were obtained on a JEOL JMS-M600 and a Shimadzu/Kratos KOMPACT MALDI I, respectively. Electron ionization mass (EIMS) spectra were measured on a JEOL JMS-DX300. UV−visible absorption spectra were recorded on a Shimadzu UV-3100PC. Elemental analyses were performed on a Perkin-Elmer model 240C elemental analyzer. Differential pulse voltammetry (DPV) was performed on a BAS CV-50W using a Ag/AgCl as a reference electrode and ferrocene/ferrocenium as an external standard.

Merck no. 5554 silica gel 60 F_{254} and Fuji Silysia BW-300 were used for TLC and silica gel flash column chromatography, respectively. All solvents and chemicals for the synthesis were of reagent grade quality, purchased commercially, and used without further purification except noted below. Pyrrole, dimethylformamide (DMF), benzene, pyridine, and toluene were distilled from calcium hydride and stored over molecular sieves. Tetrahydrofuran (THF) was distilled from benzophenone ketyl. Benzonitrile for use in the electrochemical studies was distilled from calcium hydride. Palladium on charcoal (5%) was obtained from Wako Pure Chemical Industries, Ltd. Tetrabutylammonium fluoride THF solution (1 M) was purchased from Tokyo Chemical Industry Co., Ltd. Activated manganese dioxide (<5 μm) was obtained from Aldrich Chemical Co., Inc.

Photophysical Measurements. For flash-photolysis studies, the fullerene concentrations were prepared to exhibit an optical density of at least 0.2 at 532 nm, the wavelength of irradiation. Picosecond laser flash photolysis experiments were carried out with 532-nm laser pulses from a mode-locked, *Q*-switched Quantel YG-501 DP ND:YAG laser system (pulse width ~18 ps, 2−3 mJ/pulse). The white continuum picosecond probe pulse was generated by passing the fundamental output through a D_2O/H_2O solution. Nanosecond laser flash photolysis experiments were performed with laser pulses from a Qunta-Ray CDR Nd:YAG system (532 nm, 20 ns pulse width) in a front face excitation geometry. A Xe lamp was triggered synchronously with the laser. A monochromator (SPEX) in combination with either a Hamamatsu R 5108 photomultiplier or a fast InGaAs-diode was employed to monitor transient absorption spectra.

The quantum yields were measured using the comparative method. In particular, the strong fullerene triplet−triplet absorption ($\epsilon_{700\ nm}$ = 16 100 M^{-1} cm^{-1}; $\Phi_{TRIPLET}$ = 0.98)[66] served as probe to obtain the quantum yields for the CS state, especially for the fullerene π-radical anion ($\epsilon_{1000\ nm}$ = 4700 M^{-1} cm^{-1}).[67] The quantum yields of ZnP and H_2P were determined relative to a zinc tertraphenylporphyrin standard ($\Phi_{TRIPLET}$ = 0.88).

Synthesis and Characterization. 1.[68,69] A solution of 4-methoxycarbonylbenzaldehyde (9.88 g, 60.2 mmol) and pyrrole (42.0 mL, 605 mmol) was degassed by bubbling with nitrogen for 1 h, then trifluoroacetic acid (0.12 mL, 1.6 mmol) was added. The solution was stirred for 4 h at room temperature. The mixture was diluted with benzene (300 mL), washed with 0.1 M sodium hydroxide aqueous solution and water successively, and dried over anhydrous sodium sulfate. The solvent and the unreacted pyrrole were removed under reduced pressure at room temperature. The resulting red oil was dissolved in a minimal amount of chloroform and purified by flash column chromatography on silica gel (benzene/ethyl acetate/triethylamine = 40/1/0.4 → 20/1/0.2). The main first phase was collected and evaporated under reduced pressure. Washing the residue with hexane and subsequent filtration afforded **1** as a pale grayish yellow solid (7.12 g, 25.4 mmol, 42% yield). Analytical data were identical with the reported data.[69]

2.[68,70,71] A solution of **1** (7.08 g, 25.2 mmol) and 3,5-di-*tert*-butylbenzaldehyde[72] (5.50 g, 25.2 mmol) in chloroform (2150 mL) was degassed by bubbling with nitrogen for 1 h. The reaction vessel was shielded from ambient light. Then boron trifluoride diethyl etherate (3.20 mL, 25.3 mmol) was added as one portion. The solution was stirred for 2 h at room temperature under nitrogen atmosphere. To the reddish black reaction mixture was added *p*-chloranil (9.32 g, 37.9 mmol), and the resulting mixture was stirred overnight. Triethylamine (10.6 mL, 76.1 mmol) was added, and then the reaction mixture was concentrated. Flash column chromatography on silica gel with chloroform as the eluent gave a mixture of five porphyrins including **2** and **3**.[73] Subsequent flash column chromatography on silica gel (hexane/toluene = 2/1 → 1/3) yielded the desired porphyrin from the mixture as the third band. Reprecipitation with chloroform−methanol afforded **2** as a vivid reddish purple solid (1.75 g, 1.83 mmol, 14% yield): mp > 300 °C; IR (KBr) 3316, 2955, 1722, 1607, 1592, 1476, 1434, 1362, 1278, 1248, 1113, 1022, 973, 916, 797, 764, 720 cm^{-1}; ^{1}H NMR (270 MHz, $CDCl_3$) δ −2.74 (br s, 2H), 1.52 (s, 36H), 4.11 (s, 6H), 7.80 (s, 2H), 8.07 (s, 4H), 8.31 (d, J = 8 Hz, 2H), 8.43 (d, J = 8 Hz, 2H), 8.79 (d, J = 5 Hz, 2H), 8.90 (d, J = 5 Hz, 2H); FABMS m/z 955 ($M + H^+$).

4. A mixture of **2** (500.7 mg, 524.2 μmol) in 240 mL of THF-ethanol (1:1) and potassium hydroxide (2.69 g) in water (24 mL) was refluxed for 7.5 h. After cooling, the solvent was evaporated, the residue diluted with 300 mL water, and the desired porphyrin dipotassium salt filtered. Acidification (pH 2) of an aqueous suspension of the dipotassium salt with concentrated hydrochloric acid and subsequent filtration gave **4** as a vivid reddish purple powder (473.2 mg, 510.4 mol, 97% yield): mp > 300 °C; IR (KBr) 3325, 3000 (br), 2964, 1683, 1606, 1476, 1423, 1362, 1313, 1284, 1248, 1178, 973, 917, 796, 765, 716 cm^{-1}; ^{1}H NMR (270 MHz, $CDCl_3$/DMSO-d_6 = 3/2) δ −2.82 (br s, 2H), 1.54

(64) Guldi, D. M.; Asmus, K.-D. *Radiat. Phys. Chem*. **1999**, *56*, 449.
(65) DaRos, T.; Prato, M. *Chem. Commun*. **1999**, 663.
(66) Luo, C.; Fujitsuka, M.; Watanabe, A.; Ito, O.; Gan, L.; Huang, Y.; Huang, C.-H. *J. Chem. Soc., Faraday Trans.* **1998**, *94*, 527.
(67) Luo, C.; Fujitsuka, M.; Huang, C.-H.; Ito, O. *Phys. Chem. Chem. Phys*. **1999**, *1*, 2923.
(68) Lee, C.-H.; Lindsey, J. S. *Tetrahedron* **1994**, *50*, 11427.
(69) Brückner, C.; Zhang, Y.; Rettig, S. J.; Dolphin, D. *Inorg. Chim. Acta* **1997**, *263*, 279.
(70) Lindsey, J. S.; Schreiman, I. C.; Hsu, H. C.; Kearney, P. C.; Marguerettaz, A. M. *J. Org. Chem*. **1987**, *52*, 827.
(71) Lindsey, J. S.; Wagner, R. W. *J. Org. Chem*. **1989**, *54*, 828.
(72) Newman, M. S.; Lee, L. F. *J. Org. Chem*. **1972**, *37*, 4468.
(73) Tamiaki, H.; Suzuki, S.; Maruyama, K. *Bull. Chem. Soc. Jpn*. **1993**, *66*, 2633.

(s, 36H), 7.82 (s, 2H), 8.05 (s, 4H), 8.30 (d, $J = 8$ Hz, 2H), 8.43 (d, $J = 8$ Hz, 2H), 8.83 (d, $J = 5$ Hz, 2H), 8.91 (d, $J = 5$ Hz, 2H); MALDI-TOFMS (positive mode) *m*/*z* 927 ($M + H^+$).

5. A mixture of **3** (2.5 g, 2.5 μmol) in 500 mL of 2-propanol and potassium hydroxide (14 g) in water (125 mL) was refluxed for 6 h. After cooling, the mixture was acidified with concentrated hydrochloric acid and extracted with chloroform. The organic extract was washed with saturated sodium bicarbonate aqueous solution and dried over anhydrous sodium sulfate; the solvent was then removed under reduced pressure. Flash column chromatography on silica gel (chloroform, then chloroform/methanol = 9/1) afforded **5** as a vivid reddish purple powder (1.9 g, 1.9 mmol, 76% yield): mp > 300 °C; IR (KBr) 3317, 3000 (br), 2963, 1694, 1593, 1475, 1423, 1394, 1363, 1267, 1248, 973, 915, 801, 761, 731, 715 cm^{-1}; ^1H NMR (270 MHz, $CDCl_3$) δ −2.68 (br s, 2H), 1.52 (s, 18H), 1.53 (s, 36H), 7.80 (m, 3H), 8.08 (d, $J = 2$ Hz, 2H), 8.09 (d, $J = 2$ Hz, 4H), 8.39 (d, $J = 8$ Hz, 2H), 8.54 (d, $J = 8$ Hz, 2H), 8.81 (d, $J = 5$ Hz, 2H), 8.91 (s, 4H), 8.92 (d, $J = 5$ Hz, 2H); FABMS *m*/*z* 995 ($M + H^+$).

7.[44b] A solution of zinc acetate dihydrate (5.00 g, 22.8 mmol) in methanol (100 mL) was added to a solution of 5-(4-aminophenyl)-10,15,20-tris(3,5-di-*tert*-butylphenyl)porphyrin[44b] (501.6 mg, 519.0 μmol) in chloroform (400 mL) and refluxed for 1 h. After cooling, the reaction mixture was washed with saturated sodium bicarbonate aqueous solution and water successively and dried over anhydrous sodium sulfate, and then the solvent was evaporated. Flash column chromatography on silica gel with toluene as the eluent and subsequent reprecipitation from benzene−methanol afforded **7** as a deep red purple powder (506.4 mg, 491.8 μmol, 95% yield): mp > 300 °C; IR (KBr) 3385, 2961, 1592, 1476, 1426, 1393, 1362, 1339, 1286, 1247, 1219, 1179, 1000, 929, 899, 882, 823, 798, 757, 718 cm^{-1}; ^1H NMR (270 MHz, $CDCl_3$ plus a drop of pyridine-d_5) δ 1.51 (s, 18H), 1.51 (s, 36H), 7.02 (d, $J = 8$ Hz, 2H), 7.75 (t, $J = 2$ Hz, 3H), 7.97 (d, $J = 8$ Hz, 2H), 8.05 (d, $J = 2$ Hz, 6H), 8.88−8.90 (m, 6H), 8.94 (d, $J = 5$ Hz, 2H); FABMS *m*/*z* 1028 ($M + H^+$).

8.[74] To a solution of 4-nitrobenzyl alcohol (5.65 g, 36.9 mmol) in DMF (15.0 mL), were added *tert*-butylchlorodimethylsilane (8.84 g, 58.7 mmol) and imidazole (8.29 g, 122 mmol), and then the reaction mixture was stirred for 2.5 h at room temperature under nitrogen atmosphere. The solvent was removed under reduced pressure. Flash column chromatography on silica gel (hexane/toluene = 25/75/0.3) afforded **8** as a colorless solid (9.87 g, 36.9 mmol, 100%): mp 30.5−32.5 °C; IR (KBr) 2929, 2859, 1601, 1520, 1494, 1471, 1416, 1338, 1288, 1264, 1202, 1099, 1011, 940, 840, 779, 734, 673, 640 cm^{-1}; ^1H NMR (270 MHz, $CDCl_3$) δ 0.13 (s, 6H), 0.96 (s, 9H), 4.83 (s, 2H), 7.48 (d, $J = 8$ Hz, 2H), 8.19 (d, $J = 8$ Hz, 2H); EIMS (rel intensity) *m*/*z* 267 (M^+, 70), 211 ($[M - C_4H_8]^+$, 100); Found: C, 58.64; H, 7.92; N, 5.05%. Calcd for $C_{13}H_{21}NO_3Si$: C, 58.39; H, 7.92; N, 5.24%.

9. A solution of **8** (3.32 g, 12.4 mmol) in THF (100 mL) was hydrogenated over 5% palladium on charcoal (584.9 mg) at room temperature and under atmospheric pressure until TLC analysis indicated complete reduction of **8**. The catalyst was removed by filtration, and the filtrate was concentrated under reduced pressure to give **9** as colorless oil (2.94 g, 12.4 mmol, 100%): IR (neat) 3449, 3362, 2955, 2929, 2857, 1625, 1519, 1471, 1376, 1257, 1213, 1174, 1072, 1006, 837, 777, 666 cm^{-1}; ^1H NMR (270 MHz, $CDCl_3$) δ 0.07 (s, 6H), 0.92 (s, 9H), 3.60 (br s, 2H), 4.62 (s, 2H), 6.65 (d, $J = 8$ Hz, 2H), 7.10 (d, $J = 8$ Hz, 2H); High resolution (HR) EIMS calcd for $[C_{13}H_{23}NOSi]^+$: 237.1549, found: 237.1544.

10.[46] A solution of **4** (200.7 mg, 216.5 μmol), thionyl chloride (0.310 mL, 4.25 mmol), and pyridine (0.30 mL) in benzene (30.0 mL) was refluxed for 2 h under nitrogen atmosphere. The excess reagent and solvents were removed under reduced pressure, and the residue was redissolved in a mixture of benzene (30 mL) and pyridine (1.0 mL). To the reaction mixture were added **7** (222.1 mg, 215.7 μmol) and a solution of **9** (50.5 mg, 212.7 μmol) in benzene (1.0 mL). The solution was allowed to stir overnight at room temperature under nitrogen atmosphere. TLC showed three products (R_f = 0.80, 0.43, and 0.15, chloroform) and the second band was separated by flash column chromatography on silica gel (toluene/triethylamine = 100/0.5, then toluene/ethyl acetate/triethylamine = 100/0.5/0.5 → 100/1/0.5). Reprecipitation from chloroform−acetonitrile afforded **10** as a deep reddish purple powder (157.2 mg, 72.8 μmol, 34% yield): mp > 300 °C; IR (KBr) 2962, 1673, 1645, 1592, 1524, 1495, 1474, 1368, 1317, 1248, 1074, 1000, 974, 798, 757, 716 cm^{-1}; ^1H NMR (270 MHz, $CDCl_3$) δ −2.68 (br s, 2H), 0.15 (s, 6H), 0.98 (s, 9H), 1.53 (s, 36H), 1.55 (s, 54H), 4.79 (s, 2H), 7.42 (d, $J = 8$ Hz, 2H), 7.74 (d, $J = 8$ Hz, 2H), 7.79 (s, 1H), 7.81 (s, 2H), 7.83 (s, 2H), 8.12 (s, 11H), 8.17 (d, $J = 8$ Hz, 2H), 8.24 (d, $J = 8$ Hz, 2H), 8.32−8.48 (m, 9H), 8.83 (d, $J = 5$ Hz, 2H), 8.90 (d, $J = 5$ Hz, 2H), 8.95 (d, $J = 5$ Hz, 2H), 8.98 (d, $J = 5$ Hz, 2H), 9.02−9.06 (m, 8H); MALDI-TOFMS (positive mode) *m*/*z* 2158 ($M + H^+$).

11.[74] To a solution of **10** (50.3 mg, 23.3 μmol) in THF (15 mL) was added 0.070 mL of tetrabutylammonium fluoride (1 M in THF), and then the mixture was stirred for 3.5 h at room temperature under nitrogen atmosphere. The solvents were removed under reduced pressure. Flash column chromatography on silica gel (toluene/ethyl acetate = 9/1) and subsequent reprecipitation from chloroform−acetonitrile afforded **11** as a deep reddish purple powder (38.5 mg, 18.8 μmol, 81% yield): mp > 300 °C; IR (KBr) 2962, 1682, 1592, 1515, 1494, 1477, 1363, 1314, 1248, 1000, 973, 799, 757, 717 cm^{-1}; ^1H NMR (400 MHz, $CDCl_3$) δ −2.68 (br s, 2H), 1.53 (s, 36H), 1.55 (s, 54H), 4.68 (d, $J = 5$ Hz, 2H), 7.41 (d, $J = 8$ Hz, 2H), 7.73 (d, $J = 8$ Hz, 2H), 7.79 (s, 1H), 7.81 (s, 2H), 7.84 (s, 2H), 8.08 (s, 1H), 8.11−8.13 (m, 10H), 8.17 (d, $J = 8$ Hz, 2H), 8.24 (d, $J = 8$ Hz, 2H), 8.33−8.35 (m, 4H), 8.38 (d, $J = 8$ Hz, 2H), 8.43 (d, $J = 8$ Hz, 2H), 8.47 (s, 1H), 8.82 (d, $J = 5$ Hz, 2H), 8.89 (d, $J = 5$ Hz, 2H), 8.95 (d, $J = 5$ Hz, 2H), 8.98 (d, $J = 5$ Hz, 2H), 9.03 (s, 4H), 9.06 (d, $J = 5$ Hz, 2H), 9.07 (d, $J = 5$ Hz, 2H); MALDI-TOFMS (positive mode) *m*/*z* 2044 ($M + H^+$).

12. To a solution of **11** (38.4 mg, 18.8 μmol) in chloroform (20 mL), was added at one portion activated manganese dioxide (384.2 mg, 4.42 mmol), and then the suspended mixture was stirred for 2 h at room temperature under nitrogen atmosphere. The catalyst was removed by filtration, and the filtrate was concentrated under reduced pressure. Flash column chromatography on silica gel (toluene/ethyl acetate = 50/1) and subsequent reprecipitation from chloroform−acetonitrile afforded **12** as a deep reddish purple powder (29.9 mg, 14.6 μmol, 78% yield): mp > 300 °C; IR (KBr) 2961, 1694, 1591, 1515, 1495, 1477, 1362, 1312, 1247, 1220, 1000, 973, 798, 717 cm^{-1}; ^1H NMR (270 MHz, $CDCl_3$) δ −2.68 (br s, 2H), 1.53 (s, 36H), 1.55 (s, 54H), 7.79 (s, 1H), 7.81 (s, 2H), 7.84 (s, 2H), 7.93 (br s, 4H), 8.10−8.16 (m, 12H), 8.22−8.43 (m, 12H), 8.81 (d, $J = 5$ Hz, 2H), 8.88 (d, $J = 5$ Hz, 2H), 8.95 (d, $J = 5$ Hz, 2H), 8.97 (d, $J = 5$ Hz, 2H), 9.02 (s, 4H), 9.04−9.06 (m, 4H), 9.98 (s, 1H); MALDI-TOFMS (positive mode) *m*/*z* 2042 ($M + H^+$).

ZnP−H_2P−C_{60}.[75] A solution of **12** (40.7 mg, 19.9 μmol), C_{60} (67.5 mg, 93.7 μmol), and *N*-methylglycine (83.3 mg, 935 mmol) in toluene (75 mL) was refluxed under nitrogen atmosphere until TLC analysis showed no detection of **12**. The reaction mixture was poured on the top of a flash chromatography column (silica gel) which was washed with toluene as an eluate to remove unreacted C_{60}. Then the column was washed with toluene/ethyl acetate (100/1), eluting the desired product. Reprecipitation from benzene-acetonitrile afforded **ZnP−H_2P−C_{60}** as a dark grayish purple powder (43.8 mg, 15.7 μmol, 79% yield): mp > 300 °C; IR (KBr) 2953, 1682, 1591, 1515, 1495, 1471, 1361, 1312, 1247, 1220, 1000, 973, 798, 716, 527 cm^{-1}; ^1H NMR (270 MHz, $CDCl_3$) ϵ −2.84 (s, 2H), 1.53 (s, 90H), 2.67 (br s, 3H), 3.67 (br s, 1H), 4.31 (br s, 1H), 4.50 (br s, 1H), 7.61 (br s, 2H), 7.79 (s, 3H), 7.81 (s, 2H), 7.96 (d, $J = 8$ Hz, 2H), 8.04 (s, 4H), 8.09 (s, 6H), 8.20−8.31 (m, 8H), 8.42 (d, $J = 8$ Hz, 2H), 8.48 (d, $J = 8$ Hz, 2H), 8.70 (br s, 2H), 8.77 (d, $J = 4$ Hz, 2H), 8.88−8.90 (m, 6H), 9.01−9.03 (m, 8H); MALDI-TOFMS (positive mode) *m*/*z* 2794 ($M + H^+$), (negative mode) *m*/*z* 721 (C_{60}^-); UV−vis λ_{max} (log ϵ) (THF) 350 (sh, 4.73), 361 (sh, 4.71), 404 (sh, 5.16), 420 (sh, 5.81), 427 (6.01), 485 (3.90), 516 (4.43), 555 (4.55), 597 (4.26), 649 (3.78), 704 (2.7) nm.

ZnP−H_2P. The dyad was synthesized from **4** (86.9 mg, 93.7 μmol), **7** (96.5 mg, 93.7 μmol), and 4-hexadecylaniline (30.2 mg, 95.1 μmol)

(74) Corey, E. J.; Venkateswarlu, A. *J. Am. Chem. Soc*. **1972**, *94*, 6190.

(75) Maggini, M.; Scorrano, G.; Prato, M. *J. Am. Chem. Soc*. **1993**, *115*, 9798.

by the same method as that described for **10**. **ZnP−H$_2$P** was crystallized as a deep reddish purple powder from benzene-acetonitrile (28.5 mg, 12.7 μmol, 14% yield): mp > 300 °C; IR (KBr) 2962, 2926, 2855, 1683, 1592, 1515, 1495, 1476, 1394, 1362, 1313, 1247, 1220, 1000, 973, 798, 717 cm^{-1}; ^{1}H NMR (270 MHz, $CDCl_3$) δ −2.69 (br s, 2H), 0.89 (t, J = 7 Hz, 3H), 1.27−1.80 (m, 118H), 2.65 (t, J = 7 Hz, 2H), 7.27 (d, J = 8 Hz, 2H), 7.68 (d, J = 8 Hz, 2H), 7.81−7.83 (m, 5H), 8.08 (s, 1H), 8.12 (s, 10H), 8.18 (d, J = 8 Hz, 2H), 8.25 (d, J = 8 Hz, 2H), 8.33−8.49 (m, 9H), 8.84 (d, J = 5 Hz, 2H), 8.90 (d, J = 5 Hz, 2H), 8.96 (d, J = 5 Hz, 2H), 8.98 (d, J = 5 Hz, 2H), 9.02−9.06 (m, 8H); MALDI-TOFMS (positive mode) m/z 2244 (M + H$^+$); UV−vis λ_{max} (log ϵ) (THF) 356 (sh, 4.51), 368 (4.54), 404 (sh, 5.13), 420 (sh, 5.80), 427 (5.99), 486 (3.76), 516 (4.40), 556 (4.52), 597 (4.23), 649 (3.74) nm.

15. A solution of **5** (500 mg, 0.519 mmol), thionyl chloride (0.38 mL, 5.2 mmol), and pyridine (1 mL) in benzene (100 mL) was refluxed for 1 h under nitrogen atmosphere. The excess reagent and solvents were removed under reduced pressure, and the residue was redissolved in a mixture of benzene (20 mL) and pyridine (1 mL). To the reaction mixture was added **13**[76] (215 mg, 1.04 mmol). The solution was stirred for 18 h at room temperature under nitrogen atmosphere, and then the solvent was evaporated. Flash column chromatography on silica gel with benzene as the eluent gave a mixture of **14** and **15**. The mixture was redissolved in a mixture of chloroform (50 mL), trifluoroacetic acid (20 mL), and 5% sulfuric acid (15 mL). After stirring overnight at room temperature, the mixture was poured onto 100 mL of water and extracted with chloroform. The organic extract was washed with saturated sodium bicarbonate aqueous solution and water successively, dried over anhydrous sodium sulfate, and evaporated. Flash column chromatography on silica gel with chloroform as the eluent and subsequent reprecipitation from benzene−methanol afforded **15** as a deep purple powder (270 mg, 0.253 mmol, 49% yield): mp > 300 °C; IR (KBr) 3318, 2963, 2719, 1695, 1592, 1515, 1475, 1411, 1363, 1305, 1247, 1164, 972, 915, 801, 732 cm^{-1}; ^{1}H NMR (270 MHz, $CDCl_3$) δ −2.70 (br s, 2H), 1.55 (s, 54H), 7.79 (t, J = 2 Hz, 3H), 8.01 (s, 4H), 8.07 (d, J = 2 Hz, 2H), 8.08 (d, J = 2 Hz, 4H), 8.28 (d, J = 7 Hz, 2H), 8.33 (br s, 1H), 8.41 (d, J = 7 Hz, 2H), 8.79 (d, J = 5 Hz, 2H), 8.91 (s, 4H), 8.92 (d, J = 5 Hz, 2H), 10.01 (s, 1H); FABMS m/z 1098 (M + H$^+$).

H$_2$P−C$_{60}$. The dyad was synthesized from **15** (128 mg, 0.12 mmol), C_{60} (259 mg, 0.36 mmol), and *N*-methylglycine (320 mg, 3.60 mmol) by the same method as that described **for ZnP−H$_2$P−C$_{60}$**. **H$_2$P−C$_{60}$** was isolated as a brownish black powder from chloroform−methanol (155.7 mg, 0.0844 mmol, 70% yield): mp > 300 °C; IR (KBr) 2962, 1686, 1593, 1515, 1476, 1423, 1363, 1313, 1247, 973, 914, 800, 729, 527 cm^{-1}; ^{1}H NMR (270 MHz, $CDCl_3$) δ −2.82 (br s, 2H), 1.52 (s, 54H), 2.63 (s, 3H), 3.58 (d, J = 10 Hz, 1H), 4.13 (s, 1H), 4.46 (d, J = 10 Hz, 1H), 7.55 (br s, 2H), 7.78 (s, 3H), 7.98 (d, J = 8 Hz, 2H), 8.03 (d, J = 2 Hz, 4H), 8.07 (d, J = 2 Hz, 2H), 8.18 (d, J = 8 Hz, 2H), 8.32 (d, J = 8 Hz, 2H), 8.76 (d, J = 5 Hz, 2H), 8.86 (s, 6H), 8.90 (br s, 1H); FABMS m/z 1847 (M + H$^+$), 720 (C_{60}^+); UV−vis λ_{max} (log ϵ) (THF) 366 (4.65), 405 (sh, 5.03), 420 (5.75), 484 (3.78), 516 (4.33), 550 (4.09), 593 (3.82), 649 (3.76) nm.

ZnP−C$_{60}$.[44g,h] A saturated solution of zinc acetate dihydrate in methanol (3.5 mL) was added to a solution of **H$_2$P−C$_{60}$** (70 mg, 38 μmol) in chloroform (35 mL) and refluxed for 30 min. After cooling, the reaction mixture was washed with saturated sodium bicarbonate aqueous solution and water successively, dried over anhydrous sodium sulfate, and then the solvent was removed under reduced pressure. Flash column chromatography on silica gel with chloroform as the eluent and subsequent reprecipitation from chloroform−methanol afforded **ZnP−C$_{60}$** as a dark grayish brown powder (60.8 mg, 0.0319 mmol, 84% yield): mp > 300 °C; IR (KBr) 2962, 1687, 1592, 1515, 1362, 1314, 1247, 1001, 823, 797, 717, 527 cm^{-1}; ^{1}H NMR ($CDCl_3$) δ 1.51 (s, 54H), 2.60 (s, 3H), 3.44 (br s, 1H), 3.91 (br s, 1H), 4.34 (br s, 1H), 7.49 (br s, 2H), 7.77 (m, 3H), 7.97 (d, J = 8 Hz, 2H), 8.03 (m, 6H), 8.18 (d, J = 8 Hz, 2H), 8.32 (d, J = 8 Hz, 2H), 8.86 (d, J = 5 Hz, 2H), 8.93 (s, 4H), 8.96 (d, J = 5 Hz, 2H), 8.97 (br s, 1H); FABMS m/z 1910 (M + H$^+$), 721 (C_{60}^+); UV−vis λ_{max} (log ϵ) (THF) 405 (4.80), 426 (5.88), 490 (3.52), 519 (3.70), 557 (4.41), 597 (4.05), 637 (sh, 2.8) nm.

ZnP.[44c] **ZnP** was synthesized from **H$_2$P**[44b] (43.0 mg, 42.6 μmol) by the same method as that described for **ZnP−C$_{60}$**. **ZnP** was crystallized as a deep purple microcrystalline solid from benzene−acetonitrile (36.3 mg, 33.9 μmol, 80% yield): mp > 300 °C; IR (KBr) 3318 (br), 2962, 1674, 1593, 1515, 1394, 1362, 1288, 1247, 1220, 1181, 1069, 1000, 929, 823, 798, 718 cm^{-1}; ^{1}H NMR ($CDCl_3$) δ 1.52 (s, 54H), 2.32 (s, 3H), 7.47 (s, 1H), 7.78 (m, 3H), 7.85 (d, J = 8 Hz, 2H), 8.08 (m, 6H), 8.18 (d, J = 8 Hz, 2H), 8.95 (d, J = 4 Hz, 2H), 8.99 (d, J = 4 Hz, 2H), 9.00 (s, 4H); FABMS m/z 1071 (M + H$^+$); UV−vis λ_{max} (log ϵ) (THF) 360 (sh, 4.03), 385 (sh, 3.90), 405 (4.69), 426 (5.83), 494 (sh, 3.17), 519 (3.55), 557 (4.36), 597 (4.02) nm.

C$_{60}$−Ar. C$_{60}$−Ar was prepared from C_{60}, 3,5-di-*tert*-butylbenzaldehyde, and *N*-methylglycine following the same procedures as described previously.[44f]

Acknowledgment. Part of this work was supported by the Office of Basic Energy Sciences of the Department of Energy. This is document NDRL-4175 from the Notre Dame Radiation Laboratory). Part of this work was supported by Grants-in-Aid for COE Research and Scientific Research on Priority Areas of Electrochemistry of Ordered Interfaces (No. 11118247 to H.I.) and Priority Area of Creation of Delocalized Conjugated Electronic Systems (No. 10146103 to Y.S.) from Ministry of Education, Science, Sports and Culture, Japan. Y.S. and H.I thank the Mitsubishi and Sumitomo Foundation for financial support.

JA993959Z

(76) Imahori, H.; Azuma, T.; Ajavakom, A.; Norieda, H.; Yamada, H.; Sakata, Y. *J. Phys. Chem.* **1999**, *103*, 7233.